

ECMWF Newsletter

Number 150 – Winter 2016/17

European Centre for Medium-Range Weather Forecasts
Europäisches Zentrum für mittelfristige Wettervorhersage
Centre européen pour les prévisions météorologiques à moyen terme

IFS upgrade brings sea-ice coupling

Impact of orographic drag on forecast skill

CERA-20C climate reanalysis

Wave forecast verification

© Copyright 2017

European Centre for Medium-Range Weather Forecasts, Shinfield Park, Reading, RG2 9AX, England

The content of this Newsletter is available for use under a Creative Commons Attribution-Non-Commercial-No-Derivatives-4.0-Unported Licence. See the terms at <https://creativecommons.org/licenses/by-nc-nd/4.0/>.

The information within this publication is given in good faith and considered to be true, but ECMWF accepts no liability for error or omission or for loss or damage arising from its use.

CONTENTS

EDITORIAL

A special year 1

NEWS

Flash floods over Greece in early September 2016 2
 ECMWF widens role in WMO severe weather projects 4
 New opportunities from HEO satellites 5
 Lakes in weather prediction: a moving target 6
 New Director of Research appointed 7
 New Council President elected 7
 ERA5 aids in forecast performance monitoring 8
 ECMWF to work with RIMES on flood forecasting 8
 Scientists discuss methods to simulate all-scale
 geophysical flows 9
 C3S trials seasonal forecast service 10
 Multi-decadal variability in predictive skill of the
 winter NAO 11
 ECMWF meets Ibero-American weather services 12
 Experts debate future of supercomputing in meteorology .. 13

METEOROLOGY

New IFS cycle brings sea-ice coupling and higher ocean
 resolution 14
 Impact of orographic drag on forecast skill 18
 CERA-20C: An Earth system approach to climate
 reanalysis 25
 Twenty-one years of wave forecast verification 31

GENERAL

ECMWF Council and its committees 37
 ECMWF Calendar 2017 38
 Contact information 38
 ECMWF publications 39
 Index of newsletter articles 39

PUBLICATION POLICY

The *ECMWF Newsletter* is published quarterly. Its purpose is to make users of ECMWF products, collaborators with ECMWF and the wider meteorological community aware of new developments at ECMWF and the use that can be made of ECMWF products. Most articles are prepared by staff at ECMWF, but articles are also welcome from people working elsewhere, especially those from Member States and Co-operating States. The *ECMWF Newsletter* is not peer-reviewed.

Editor: Georg Lentze

Typesetting and Graphics: Anabel Bowen with the assistance of Simon Witter

Any queries about the content or distribution of the *ECMWF Newsletter* should be sent to Georg.Lentze@ecmwf.int

Guidance about submitting an article is available at www.ecmwf.int/en/about/news-centre/media-resources

CONTACTING ECMWF

Shinfield Park, Reading, Berkshire RG2 9AX, UK
 Fax: +44 118 986 9450
 Telephone: National 0118 949 9000
 International +44 118 949 9000
 ECMWF website: www.ecmwf.int

A special year

In number theory, 2017 is a special type of prime which can be written as the sum of two squares as it is congruent to 1 modulo 4, based on Fermat's Christmas theorem. A special number for a very special year, and I want to wish all of you a great start to what will no doubt be a special year for all of us.

For ECMWF, 2017 is the first full year of implementing the *Strategy 2016–2025: the Strength of a Common Goal*. It brings with it all the excitement that comes with the early stages of such an ambitious plan. The year will be marked by many important moments for the Centre: 25 years of ensemble prediction, leading up to the primacy of probabilistic prediction in our new Strategy; tests to define the best possible configuration of the 5 km ensemble planned for 2025; the release of the seasonal System 5, which will be a step towards seamless prediction, bringing forecasts similar in resolution to our monthly forecasts; progress in the ERA5 climate reanalysis, which is expected to cover the period up to 2010 by the end of 2017; and two scheduled upgrades of the Integrated Forecasting System (IFS).

As usual, all this will happen through collaboration with the national meteorological services of our Member and Co-operating States and with the wider meteorological community. Recent examples of the fruits of this collaboration, featured prominently in this Newsletter, include the introduction into the IFS of the interactive sea-ice model LIM2 developed at the Belgian Université Catholique de Louvain and of the higher-resolution ocean model based on the community model NEMO.

Our supercomputer is also a clear and strong symbol of the spirit of collaboration that is at the heart of ECMWF. This is of course where we develop and test our science, and where we produce our forecasts. But some of ECMWF's High-Performance Computing Facility (HPCF) is also available for use by our Member States. It is clear that we have now reached the maximum capacity at our headquarters in Reading as implementing the Strategy will require an increase in computing power of at least one order of magnitude.

Whilst technological advances as well as the efficiency gains made through our Scalability Programme will help, ultimately a new site for a larger HPCF will be needed. After visits to potential sites in several Member States, we are now approaching the crucial moment when our Council will decide where to relocate ECMWF's Data Centre. This decision, which marks a critical moment for ECMWF's future, will be taken at the end of February at an extraordinary Council session.

We are confident that once again the spirit of cooperation will prevail and will drive our governing body's choice towards a solution which will maintain ECMWF as a common asset and a source of pride.

Florence Rabier
 Director-General

Flash floods over Greece in early September 2016

**TIM HEWSON,
IVAN TSONEVSKY**

Between about midday on 6 September and midday on 7 September 2016, extreme rainfall affected parts of Greece, most notably in the southern part of the Peloponnese and also much further north, over and just south of Thessaloniki. According to media reports, the resulting flash floods caused four fatalities, invaded properties, closed roads, and caused cars to be piled up and locally swept out to sea. Rainfall reports are limited, though Kalamata airport recorded more than 130 mm in 24 hours, whilst various unofficial reports from nearby suggest 24-hour totals of the order of 200 mm, most of which fell in two or three hours. Meanwhile a report in the ESSL (European Severe Storms Laboratory) database indicates that over 300 mm fell locally near Thessaloniki. Experience from similar extreme rainfall events suggests that spatial variability can be very high. This means that even larger amounts may have accumulated very locally in each case, even in the absence of topographic forcing. In the figure showing observed rainfall totals there is evidence of such variability near Thessaloniki and also in the high-density observations over the heel of Italy, in a relatively flat area. One current project at ECMWF aims to automatically predict the degree of sub-grid variability in precipitation totals, in recognition of how important this is to users interested in flood risk, and because raw model output provides only a grid-box average.

Synoptic situation

The synoptic situation over Greece on 6 and 7 September was characterised by moist and very unstable south to south-easterly flow, ahead of upper and surface low pressure systems situated to the west. The mean 500 hPa geopotential height field from the 96-hour ensemble forecast (ENS) shown in the figure is quite accurate compared to the analysis; most notably the cut-off upper vortex – the driver of the bad weather – was well positioned over southern Italy. The equivalent high-

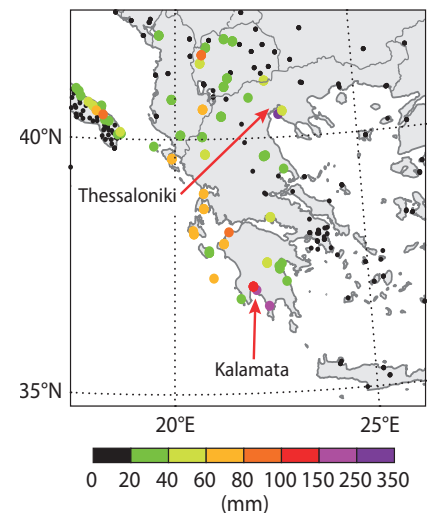


Aftermath. The floods left cars piled up in the streets of Kalamata on 7 September. (Photo: EPA/Nikitas Kotsiaris)

resolution forecast (HRES) for the same time (not shown) was very similar, just marginally worse. Getting features of the large-scale flow pattern reasonably correct is a necessary but not sufficient condition for accurate predictions of severe surface weather. The cold front shown in the inset was also a key player – extreme convective activity would lie on and ahead of it. In the model sounding in the second inset one can see evidence of extreme convective instability, given triggering by sea-surface temperatures of about 26°C, and the copious low-level moisture supply, both of which would help to generate very large rainfall totals.

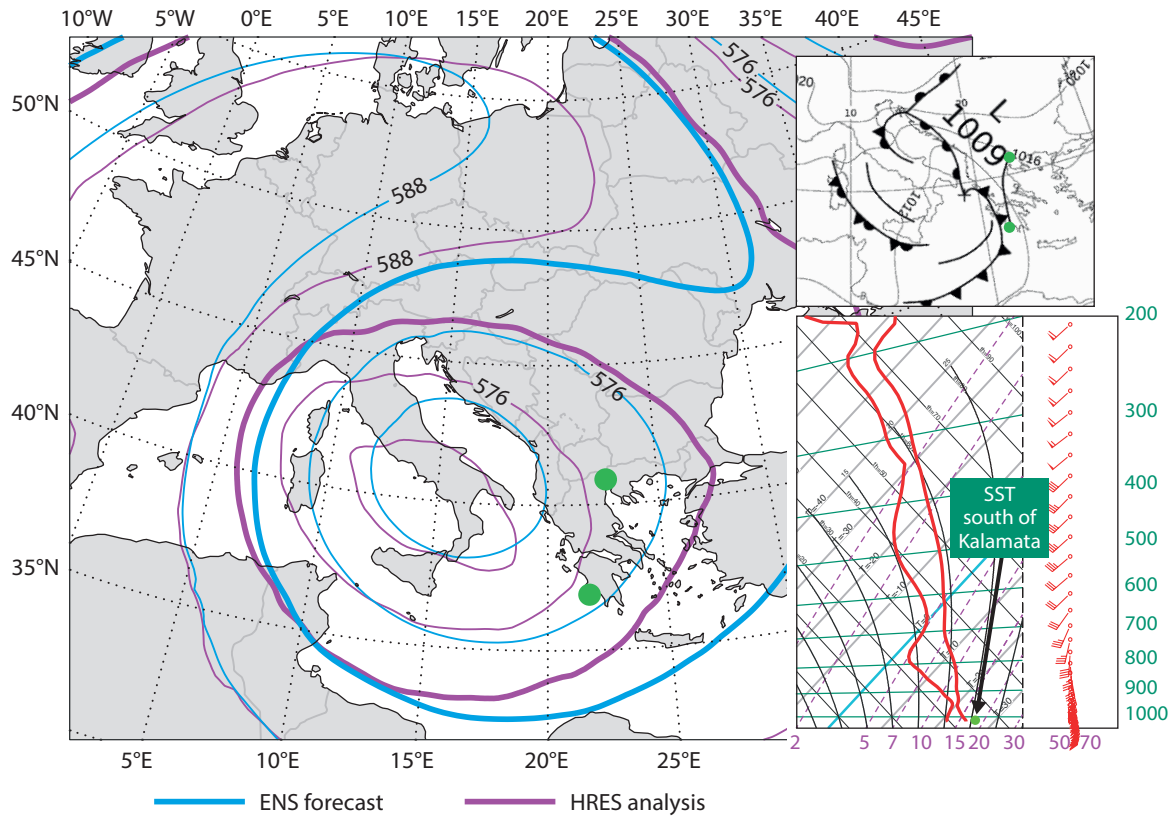
Rainfall forecasts

The remaining figures show HRES and ENS rainfall forecasts, respectively, for a lead time of three to five days, spanning the event. This relatively long window was used to be sure to capture the passage of any extreme rainfall related to the front, and also because it is a standard time window used for the EFI/SOT (Extreme Forecast Index and Shift Of Tails) products provided to forecasters on the web. HRES shows a lot of local detail, correctly signalling a potential for very large totals around Thessaloniki. However, the forecast for Kalamata does not look that extreme relative to other areas (41 mm spot total for the town). ENS as represented by ECMWF's extreme weather indices, on

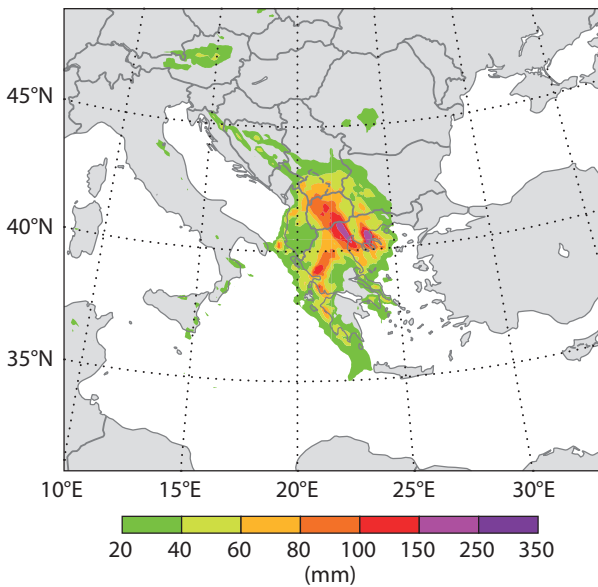


Rainfall totals. Observed 24-hour rainfall totals up to 06 UTC on 7 September 2016, compiled from both official and unofficial sources.

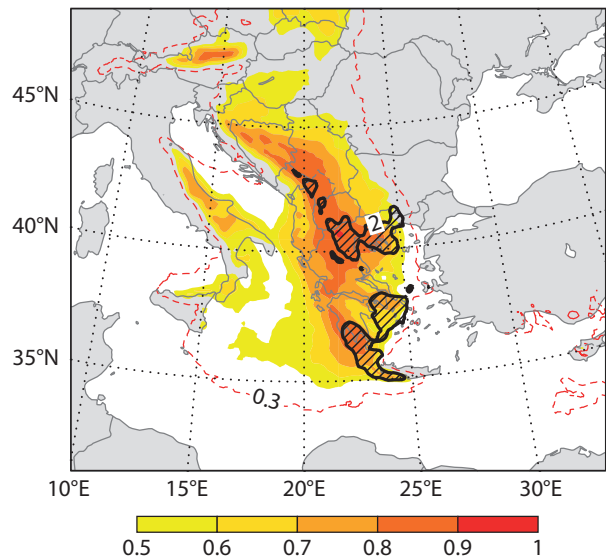
the other hand, correctly highlights both Thessaloniki and Kalamata as being at risk. The EFI is high in both locations (0.8 to 0.9), suggesting that *very large rainfall totals are likely*, whilst the SOT is also high (>2), suggesting that a *truly exceptional event is possible*. This case is a good example of the benefits of using ECMWF output and products for severe weather prediction. It also illustrates that, in the medium range at least, ENS is the main tool to use by forecasters when it comes to identifying areas at risk. HRES is more prone to provide unreliable local detail and similarly to jump between successive runs in its



Synoptic situation. The main panel shows the ENS mean 96-hour forecast of 500 hPa geopotential height valid at 00 UTC 7 September 2016 and the HRES analysis for the same time. The top inset shows the UK Met Office surface analysis for the same time. The green dots show the location of Kalamata and Thessaloniki. The bottom inset shows a model T+0 sounding from HRES for the same time, for a marine area just south of Kalamata.



HRES rainfall forecast. HRES forecast of 72-hour rainfall total initialised at 00 UTC on 3 September 2016, valid from 00 UTC on 5 September to 00 UTC on 8 September.



EFI and SOT for rainfall. EFI (shading) and SOT (hatching for SOT>2) for 72-hour rainfall from the ENS run initialised at 00 UTC on 3 September 2016, valid from 00 UTC on 5 September to 00 UTC on 8 September.

indications of where extreme weather may be. This is especially true when the situation is dynamically and/or thermodynamically unstable, as is the case with most severe weather events,

including the one illustrated here. It is for such reasons that ensemble prediction lies at the heart of ECMWF's new ten-year Strategy. ECMWF acknowledges the use of some

rainfall data from ESSL, from the Remote Sensing Department and the Department of Meteorological Stations in the Hellenic National Meteorological Service, and from the Weather Underground website.

ECMWF widens role in WMO severe weather projects

ANNA GHELLI, CIHAN SAHIN

ECMWF has started to provide forecast products to three more regions taking part in the Severe Weather Forecasting Demonstration Project (SWFDP) run by the World Meteorological Organization (WMO). The project aims to strengthen the capacity of national meteorological and hydrological services (NMHSs) in developing and least developed countries to deliver improved forecasts and warnings of severe weather to save lives, livelihoods and property. The SWFDP is implemented as a number of regional subprojects and uses a 'cascading forecasting process' (global to regional to national). ECMWF participates as a global numerical weather prediction (NWP) centre, providing graphical products derived from ensemble and high-resolution forecasts for the domains of each regional project. Participants in these projects can access the forecast

charts available via ECMWF's website (login required).

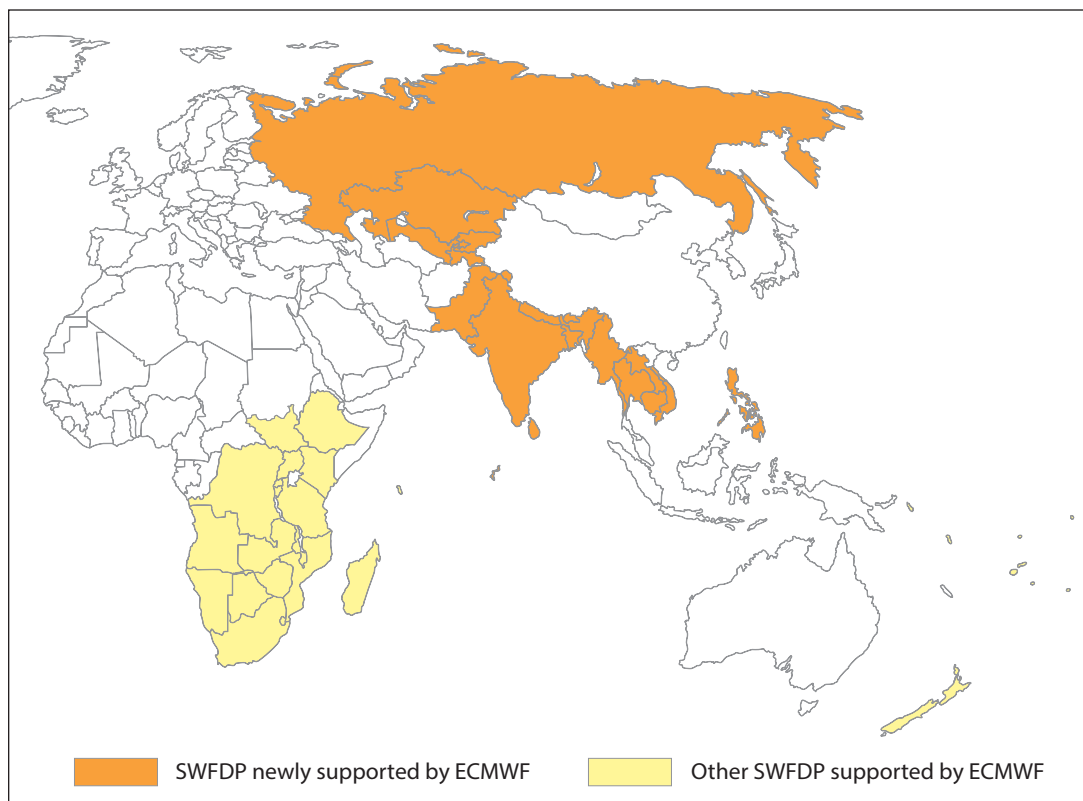
ECMWF contributes to all six SWFDP regional subprojects: Southern Africa, South Pacific, Eastern Africa, Central Asia, Bay of Bengal and Southeast Asia. In 2016, dedicated areas for the three latter subprojects (Central Asia, Bay of Bengal and Southeast Asia) were created on the website. They offer easy access to forecast products using the ecCharts framework.

As part of efforts to maximise the impact ECMWF products have on SWFDP countries, a WMO Fellow from the NMHS of Vietnam started a 12-month visit in September 2016. Vietnam is a regional centre for the Southeast Asia SWFDP. The main focus of the visit will be on the verification of ensemble products for Vietnam and the Southeast Asia SWFDP region, with an emphasis on ECMWF products provided for the SWFDP. The work will also review the use of ensemble forecasts in operational forecasting

in the region, and in particular their interpretation for severe weather event forecasts. The use of local observations available to the Vietnam NMHS and the experience of the Fellow in operational forecasting for Southeast Asia will help ECMWF to improve its understanding of model behaviour in the region.

ECMWF has also supported the SWFDP by participating in training activities. Lectures and practical activities have been provided for SWFDP Eastern Africa (November 2015, Addis Ababa, Ethiopia); West Africa (webinar in December 2015, Dakar, Senegal); SWFDP Central Asia (webinar in February 2016, Almaty, Kazakhstan); and SWFDP Bay of Bengal (webinar July 2016).

In 2017, ECMWF will seek to continue to support the Southern Africa subproject as it moves to the operational phase. In the longer term, it will work with WMO to provide enhanced training support for the SWFDP.



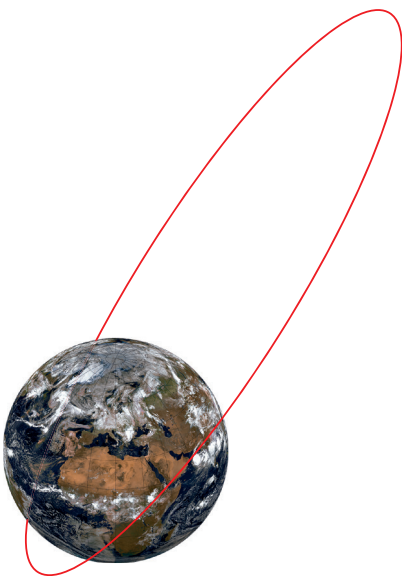
Countries participating in the Severe Weather Forecasting Demonstration Project. Regional subprojects cover Southern Africa, Eastern Africa, the South Pacific, Central Asia, the Bay of Bengal and Southeast Asia. In 2016, ECMWF created dedicated areas on its website for the three latter projects.

New opportunities from HEO satellites

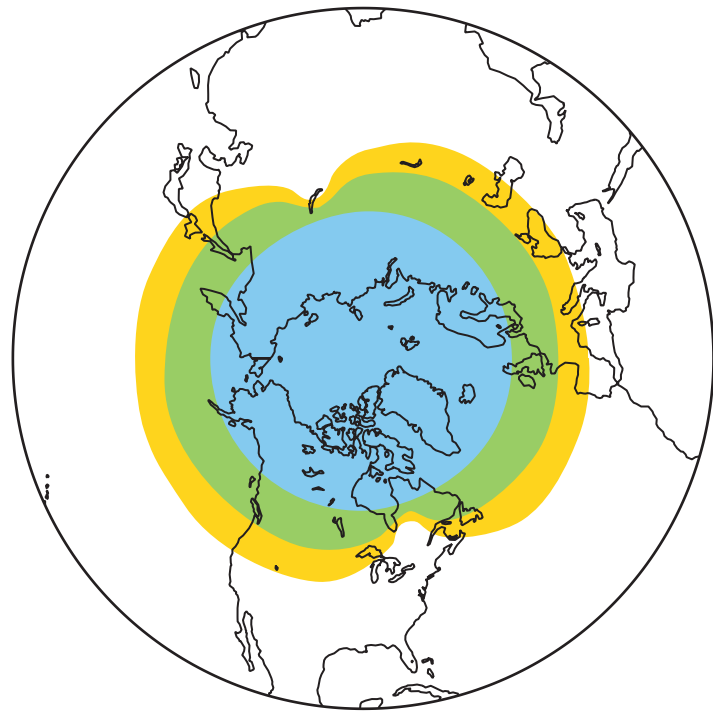
ERIK ANDERSSON,
NIELS BORMANN, KATIE LEAN

The European Organisation for the Exploitation of Meteorological Satellites (EUMETSAT) and the European Space Agency (ESA) are considering the prospects for observations from satellites in a highly elliptical orbit (HEO). This is a new opportunity that could bring weather imaging capabilities to the Arctic and high latitudes of similar quality to what is currently available in the tropics and mid-latitudes from geostationary satellites. Two such imagers in HEO would provide full and frequent coverage at high latitudes of clear benefit to numerical weather prediction (NWP). ECMWF is therefore supportive of the new mission concept.

At a recent EUMETSAT HEO meeting, the participants agreed to support an HEO mission. However, further investigations are needed to establish the user requirements for such a mission in terms of instrument capabilities, and to substantiate the benefits as a complement to a baseline polar-orbiting constellation.



Highly elliptical orbit. Satellites in highly elliptical orbits move more slowly in high-altitude parts of the orbit than in low-altitude parts, thus maximising viewing times over high latitudes. (Earth image: EUMETSAT)



■ Constant ■ 95% of the time ■ 90% of the time

Satellite coverage. Two imagers in highly elliptical orbits would provide good coverage over the North polar region. The illustration shows one possible scenario, with the actual coverage dependent on the final choice of orbit.

Furthermore, the performance and value of a dedicated HEO mission versus a hosted payload on a telecommunications satellite would have to be analysed in detail.

There is a recognised gap in the global observing system at latitudes between 50–70°N regarding the provision of tropospheric winds in the form of Atmospheric Motion Vectors (AMVs) derived from cloud and water vapour image sequences. This gap corresponds to a gap in coverage between winds provided by geostationary satellites (GEO) on the one hand and polar wind products from Low Earth Orbit (LEO) satellites on the other.

Whilst this gap can be mitigated by other satellite observation techniques combining images from multiple satellites, the data quality is lower than that from GEO and the quality expected from HEO. Furthermore, the temporal and spatial coverage is limited, leading to areas still sparse in data for each data assimilation cycle. The value of high-latitude winds is well

established through the recent addition of further polar AMV data at ECMWF and data denial experiments at other NWP centres. The inclusion of such winds is also believed to have been effective in reducing forecast busts. These investigations also confirm that operational NWP systems are not yet saturated with high-latitude good-quality wind observations. Forecasts of high-impact weather events such as cold-air outbreaks and polar lows are expected to benefit from improved observations in the Arctic.

Whilst the provision of good-quality wind observations is seen as the primary benefit HEO missions would bring, other benefits are anticipated from much-improved snow and ice monitoring capabilities and radiance assimilation. With respect to regional NWP and limited-area modelling, there is an increased need for high spatial and temporal resolution observations as the model domains expand further north, in response to the increased economic exploitation of the Arctic.

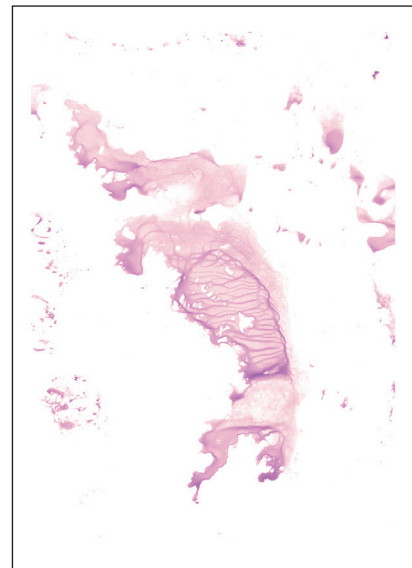
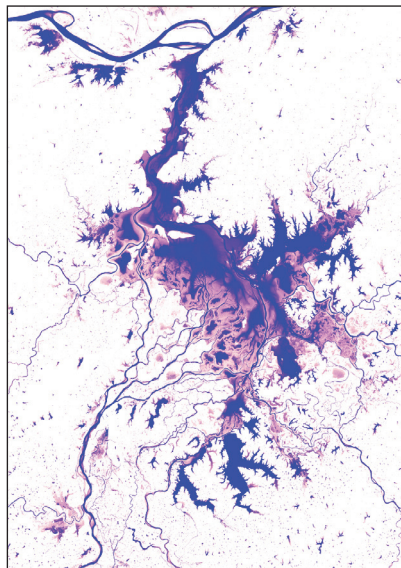
Lakes in weather prediction: a moving target

**GIANPAOLO BALSAMO (ECMWF),
ALAN BELWARD**
(Joint Research Centre)

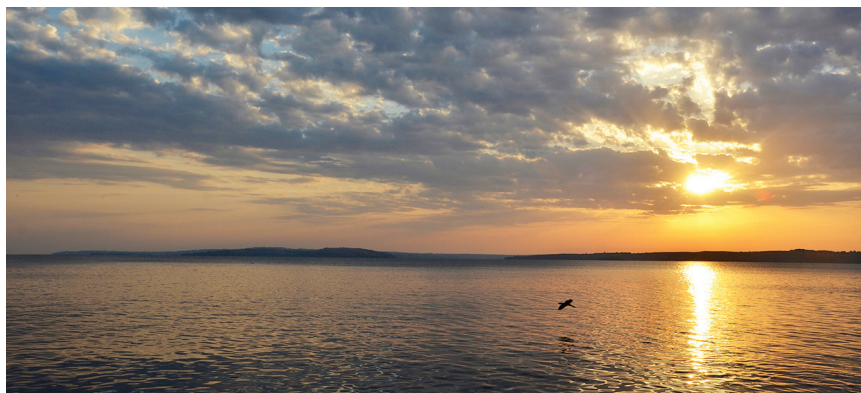
Lakes are important for numerical weather prediction (NWP) because they influence the local weather and climate. That is why in May 2015 ECMWF implemented a simple but effective interactive lake model to represent the water temperature and lake ice of all the world's major inland water bodies in the Integrated Forecasting System (IFS). The model is based on the version of the FLake parametrization developed at the German National Meteorological Service (DWD), which uses a static dataset to represent the extent and bathymetry of the world's lakes.

However, new data obtained from satellites show that the world's surface water bodies are far from static. By analysing more than 3 million satellite images collected between 1984 and 2015 by the USGS/NASA Landsat satellite programme, new global maps of surface water occurrence and change with a 30-metre resolution have been produced. These provide a globally consistent view of one of our planet's most vital resources, and they make it possible to measure where the world's surface water bodies really can be found at any given time.

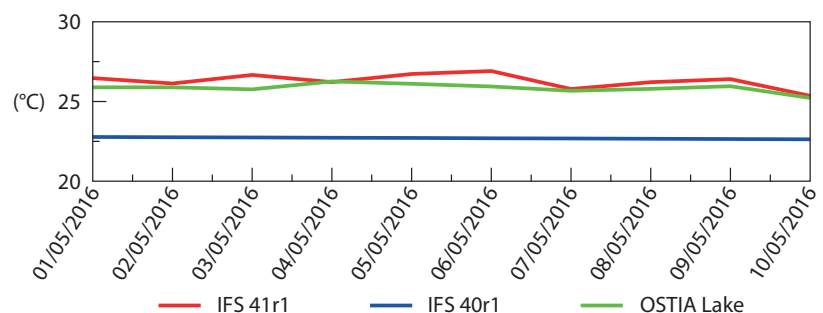
As explained in a recent *Nature* article (doi:10.1038/nature20584), the maps show that over the past three decades almost 90,000 km² of the lakes and rivers thought of as permanent have vanished from the Earth's surface. That is equivalent to Europe losing half of its lakes. The losses are linked to drought and human activities, including river diversion or damming and unregulated withdrawal. Elsewhere, more than 180,000 km² of new permanent bodies of water have come into being. Many of these are new reservoirs created around the world, others are the result of climate change. For example, the high-elevation lakes throughout the Tibetan Plateau (Earth's 'third pole') have expanded in size and number over the past decade. Some 8,000 km² of land in the area is now under water, an increase in lake area of 20%. Around the world over 20 countries have each gained at least



Dynamic lakes. The size of Poyang Lake (left), one of China's largest lakes, fluctuates dramatically between wet and dry seasons each year while overall decreasing. Lake Gairdner in Australia (right), which is over 150 km long, is an ephemeral lake resulting from episodic inundations. Both maps show the occurrence of water over the past 32 years: the lighter the tone the lower the occurrence. (Images: Joint Research Centre/Google 2016)



Lake Victoria. Lakes in tropical areas are linked with high-impact weather by contributing to the formation of convective cells. (Photo: MHGALLERY/iStock/Thinkstock)



Interactive lake model. The lake model introduced with IFS Cycle 41r1 in May 2015 is able to represent lake water temperature much better than was possible in IFS Cycle 40r1. The plot illustrates this for Lake Victoria by showing surface water temperature between 1 and 10 May 2016 in 41r1 and 40r1 analyses and according to independent satellite observations from the UK Met Office's OSTIA Lake product.

1,000 km² of new surface water.

Building on this 32-year history constructed from archived satellite imagery, the EU-funded Copernicus Earth observation services are examining ways of building a real-time monitoring system employing both the Landsat data and images from Europe's Sentinel satellites. This could help to model the impact of lakes on weather and climate and vice versa much better than is possible at present.

In the IFS, the lake model takes into account all inland waterbodies occupying at least 1% surface area of each model grid box. That corresponds to between about 1 and 3 km² of water for high-resolution and ensemble forecasts, respectively. Including lakes in ECMWF's land-atmosphere model has had a positive impact on forecasts of near-surface parameters such as temperature and precipitation in the vicinity of lakes. This is because the presence of lakes has a range of effects on weather and climate:

- Over mid-latitude regions, lakes help to foster mild micro-climate conditions by acting as thermal inertial bodies, and they trigger locally higher precipitation rates. This happens especially when lakes are shielded by mountainous regions, which is often the case given the geomorphological origin of many lakes. The Lago Maggiore area straddling Switzerland and Italy is a case in point.
- At high latitudes, lakes tend to freeze almost every winter. It is important to predict when that happens as freezing changes the surface albedo and thermal capacity, which affects the surface fluxes exchanged with the atmosphere. In winter conditions this can make the difference between light or heavy snowfall downwind from a lake, as is often seen in the vicinity of the Great Lakes.
- An accurate representation of lakes is also essential in temperate and tropical areas, where lakes are linked with

high-impact weather by contributing to the formation of convective cells. This happens mostly at nighttime due to moisture convergence and breeze effects. An example of where this regularly occurs is Lake Victoria, one of the African Great Lakes.

But accurately representing lakes in models relies on correctly mapping their geographic limits. This is where the Copernicus programme is going to help. ECMWF will therefore work with Copernicus services to explore how numerical weather prediction can benefit from the real-time monitoring of inland surface water bodies. A more dynamic representation of lakes will be part of wider moves at ECMWF towards an Earth system approach to forecasting. In line with the Centre's new Strategy for 2016–2025, such an approach takes into account the interactions between all components of the Earth system that are relevant to NWP, at the necessary level of complexity.

New Director of Research appointed



In December 2016, Dr Andrew Brown was appointed as ECMWF's next Director of Research after Professor Erland Källén steps down on 31 July 2017. Dr Brown is the Director of Science at the UK Met Office. He has extensive experience of scientific and corporate leadership, developing

strategies and partnerships and co-ordinating the work of many teams to successfully deliver scientific advances. His scientific contributions cover a variety of topics relating to atmospheric physical processes, parametrization and weather and climate modelling.

Andrew Brown. ECMWF's Council approved Dr Brown's appointment in December 2016.

New Council President elected

In December 2016, ECMWF's Council elected Professor Jorge Miguel Alberto de Miranda (Portugal) as its President and Professor Juhani Damski (Finland) as its Vice-President, both for a first term of office of one year. Professor Miranda is the President of Portugal's national meteorological service,

the Portuguese Institute for Sea and Atmosphere. He is well known at ECMWF, having served as the Council Vice-President from December 2013 to December 2016. Professor Damski is the Director General of the Finnish Meteorological Institute.

Jorge Miguel Alberto de Miranda. ECMWF's Council unanimously elected Professor Miranda as its new President in December 2016.



ERA5 aids in forecast performance monitoring

THOMAS HAIDEN, MARTIN JANOUSEK, HANS HERSBACH

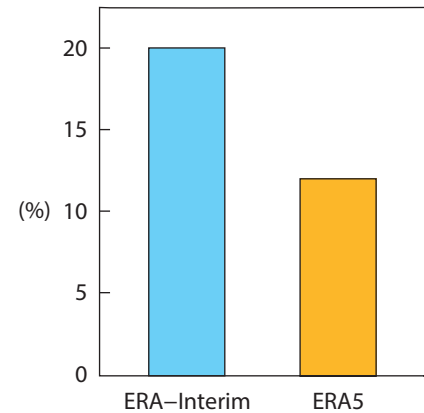
ECMWF's fifth-generation reanalysis, ERA5, provides a new reference for quantifying gains in forecast skill in the Integrated Forecasting System (IFS). For more than a decade ERA-Interim has been used to separate variations in atmospheric predictability from changes in predictive skill due to improvements of the forecasting system. However, the 9 km resolution of the high-resolution forecast (HRES) is now almost an order of magnitude higher than that of ERA-Interim (80 km), and the two versions of the forecasting system (IFS Cycles 43r1 and 31r2) differ substantially. Furthermore, ERA-Interim cannot respond to some of the changes in the observing system that have occurred over the years. This has led to an increasing divergence of the ways in which the two systems respond to variations in predictability, especially for near-surface parameters such as 2 m temperature and 10 m wind speed, and it adds some uncertainty to the assessment of long-term trends in HRES skill.

ERA5 uses IFS Cycle 41r2, which was operational until 21 November 2016, with a horizontal grid spacing of 31 km.

It uses 137 levels in the vertical, which is the same as the current HRES. For more details on ERA5, see ECMWF Newsletter 147. Since ERA5 is much closer to the current operational configuration than ERA-Interim, it provides an improved means of assessing the effect of variations in atmospheric predictability on HRES scores.

One way of quantifying the ability of a reference forecast to capture the effect of atmospheric variability on HRES skill is to determine the correlation of daily scores between the two forecasts. Note that when the correlation is computed over a period which contains one or more model upgrades, the mean value of the score over each sub-period covering the respective cycles is subtracted first. This ensures that the correlation measures the degree of correspondence relative to atmospheric variability and is not affected by step-wise changes in skill due to model upgrades.

Results for 2-metre temperature at forecast day 5 in the extratropics, using the root-mean-square error (RMSE) as a metric, show that ERA-Interim captures 80% of the day-to-day variance in HRES scores, while for ERA5 this number increases to 88%. This reduction of the 'unexplained'



Reduction in unexplained variance. ERA5 is better than ERA-Interim at capturing the day-to-day variance in IFS skill scores. For 2-metre temperature at forecast day 5 in the extratropics, the 'unexplained' variance of the RMSE for recent IFS cycles is reduced from 20% in ERA-Interim to 12% in ERA5.

variance from 20% to 12% facilitates the interpretation of the time evolution of operational scores.

These first results are based on a limited period of ERA5 forecasts (June 2014 to October 2016). When data for a longer period becomes available in 2017, more comprehensive tests will be possible, and ERA5 will eventually replace ERA-Interim as the main reference forecast in the operational evaluation of forecast skill.

ECMWF to work with RIMES on flood forecasting

REBECCA EMERTON

RIMES, the Regional Integrated Multi-Hazard Early Warning System for Asia and Africa, and ECMWF have had a cooperation agreement for the exchange of information and expertise since 2012, and recent discussions have led to further collaboration on flood forecasting. The purpose of RIMES is to provide early warning services for enhanced preparedness, response, and mitigation of natural hazards, according to the different needs of its Member States. One aspect of this is flood forecasting, in particular for flood events that occur across country borders. Cross-border rivers in



Participants at the regional training workshop. ECMWF scientist Rebecca Emerton attended on behalf of ECMWF (seated second from right).

Asia include the Ganges, Brahmaputra, Meghna, Indus and Mekong rivers, and there is an urgent need to build capabilities for the forecasting of transboundary flood events.

GloFAS, the Global Flood Awareness System, has the potential for use in forecasting such events since it combines ECMWF’s medium-range weather predictions with a hydrological model to provide probabilistic flood forecasts for the global river network.

A regional training event for flood forecasting in transboundary river basins, organised by RIMES and UN-ESCAP (United Nations Economic and Social Commission for Asia and the Pacific), was held at the Asian Institute of Technology, Thailand, from 3 to 7 October 2016. It was attended by meteorologists and hydrologists from six countries in the region alongside

representatives from several other international organisations. At this workshop, RIMES highlighted the work they are doing with GloFAS, and delegates presented aspects of flood forecasting in each country. Nepal-based hydrologist Mr Binod Parajuli demonstrated how GloFAS had been used successfully alongside existing forecasting capabilities to forecast a severe flood event in Nepal this monsoon season.

ECMWF’s role in the training workshop was to provide an interactive training session on using GloFAS forecasts, and to discuss collaboration on flood forecasting with RIMES Director Mr A.R. Subbiah. Moving forward, ECMWF and RIMES will work together to continue improving GloFAS forecasts and work towards integrating GloFAS into the existing national and regional forecasting capabilities in countries across the region.

RIMES has recently been evaluating GloFAS forecast skill in two river basins in Nepal and Myanmar. Preliminary results are promising and, going forward, RIMES will expand the evaluation to cover river basins in each country they are working with – potentially up to about 50 countries across Asia and eastern Africa. ECMWF will provide RIMES with past GloFAS forecasts for evaluation and, on the basis of the evaluation results, real-time forecast data. RIMES is also looking to work closely with its Member States in order to provide ECMWF with observed river data from countries across the region. ECMWF will use this data to calibrate GloFAS and thus further improve the forecasts.

Both ECMWF and RIMES are excited to continue collaborating to further improve forecast and early warning capabilities for transboundary flood events across the region.

Scientists discuss methods to simulate all-scale geophysical flows

CHRISTIAN KÜHNLEIN, WILLEM DECONINCK, PIOTR SMOLARKIEWICZ, NILS WEDI

From 3 to 6 October 2016, a workshop on numerical and computational methods for the simulation of all-scale geophysical flows took place at ECMWF. The event aimed to foster interdisciplinary research by bringing together scientists working on a range of numerical model developments relevant to numerical weather prediction. The scientific background of the participants ranged from small-scale turbulent flows, weather and climate to solar physics. The emphasis was on numerical solutions and dynamical core formulations, coupling to physical parametrizations and energy-efficient parallel computing.

Dynamical core formulations and numerical techniques for future non-hydrostatic Earth system modelling was one of the key topics discussed. Further contributions highlighted progress with regard to the EU-funded ESCAPE project (Energy-efficient Scalable Algorithms for Weather Prediction at Exascale). More details on ESCAPE can

$$\frac{\partial \mathcal{G} \rho}{\partial t} + \nabla \cdot (\mathbf{v} \mathcal{G} \rho) = 0$$

$$\frac{\partial \mathcal{G} \rho \mathbf{u}}{\partial t} + \nabla \cdot (\mathbf{v} \mathcal{G} \rho \mathbf{u}) = \mathcal{G} \rho \left(-\Theta_d \tilde{\mathbf{G}} \nabla \varphi' - \frac{\mathbf{g}}{\theta_a} (\theta' + \theta_a (\epsilon q'_v - q_r - q_r)) - \mathbf{f} \times \left(\mathbf{u} - \frac{\theta'}{\theta_a} \mathbf{u}_a \right) + \mathbf{M}(\mathbf{u}) + \mathbf{D} \right)$$

$$\frac{\partial \mathcal{G} \rho \theta'}{\partial t} + \nabla \cdot (\mathbf{v} \mathcal{G} \rho \theta') = \mathcal{G} \rho \left(-\tilde{\mathbf{G}}^T \mathbf{u} \cdot \nabla \theta_a - \frac{L}{c_p \pi} \left(\frac{\Delta q_{vs}}{\Delta t} + E_r \right) + \mathcal{H} \right)$$

$$\frac{\partial \mathcal{G} \rho q_k}{\partial t} + \nabla \cdot (\mathbf{v} \mathcal{G} \rho q_k) = \mathcal{G} \rho \mathcal{R}^{q_k}$$

$$\frac{\partial \mathcal{G} \rho \varphi'}{\partial t} + \nabla \cdot (\mathbf{v} \mathcal{G} \rho \varphi') = \mathcal{G} \rho \sum_{\ell=1}^3 \left(\frac{a_\ell}{c_\ell} \nabla \cdot \zeta_\ell (\tilde{\mathbf{v}} - \tilde{\mathbf{G}}^T \mathbf{C} \nabla \varphi') \right) + b_\ell \varphi' + c$$

be found at www.ecmwf.int/escape. A prominent topic was the methods employed in the finite-volume module (FVM) being developed for ECMWF’s Integrated Forecasting System (IFS). The FVM is an alternative dynamical core formulation with a finite-volume spatial discretisation that is inherently conservative and operates on a compact local stencil minimising communication distance. For more details, see ECMWF Newsletter No. 145, pp. 24–29.

The FVM is being developed under the auspices of the PantaRhei project (FP7/2012/ERC Advanced Grant agreement no. 320375) hosted at

ECMWF. The workshop was the first major dissemination of PantaRhei outcomes. For Dr Smolarkiewicz, it continues a long-standing tradition of sharing interdisciplinary research results using the finite-volume MPDATA approach in many different numerical applications covering a huge range of scales, from millimetres to hundreds of thousands of kilometres, and from seconds to millennia.

All presentations are available for download at www.ecmwf.int/en/learning/workshops-and-seminars/workshop-numerical-and-computational-methods-simulation-all-scale-geophysical-flows.

C3S trials seasonal forecast service

ANCA BROOKSHAW

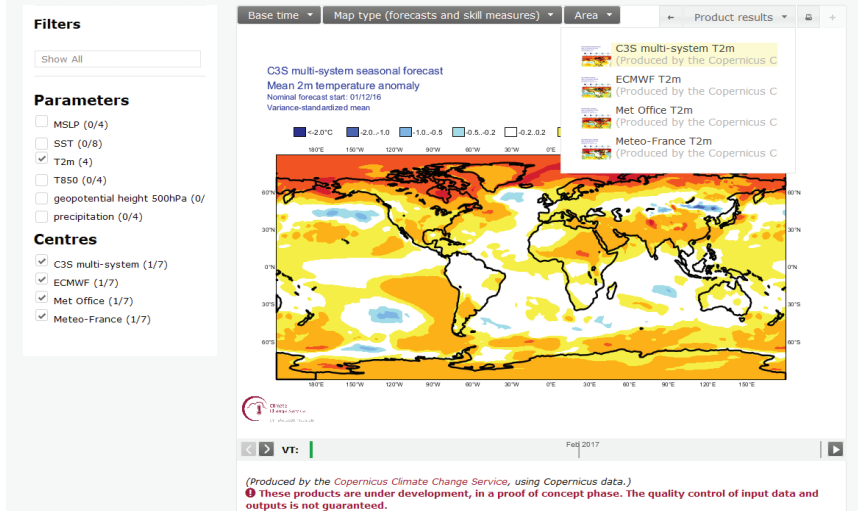
The EU-funded Copernicus Climate Change Service (C3S) operated by ECMWF has begun to trial a prototype seasonal forecast service on its website. The aim of the service is to generate seasonal forecast products based on the best information available, to an operational schedule, and to make them publicly available.

The seasonal forecast service is based on a multi-system framework. Data is collected from several European centres which either already have well-established activities in seasonal forecasting (core providers) or are committed to developing and implementing such systems into operations over the next year (additional providers). The core providers – ECMWF, the UK Met Office and Météo-France – have been delivering data to C3S for the last few months. A suite of products has been implemented at ECMWF to process this data into forecast products of relevance to users. The additional providers – CMCC (Italy's Euro-Mediterranean Center on Climate Change) and DWD (Germany's National Meteorological Service) – will start submitting data for inclusion in the product suite in the course of 2017.

Staged implementation

As the driving principle behind the seasonal forecast service is relevance to users, the service will be developed and implemented in several stages. To begin with, products with which users of seasonal forecasts are already familiar have been created and published. Feedback on these initial releases will be used alongside information collected in separate, independent user requirement-gathering activities to refine and enhance the portfolio of products. To allow access to the prototype service as early as possible, the initial releases come with a limited amount of documentation and information on the quality of the products. During the trial period, we recommend using the contributing institutions' own documentation for supporting information. In the next release C3S will calculate and display skill information for the suite of products provided.

C3S seasonal charts



Multi-system forecasts. A prototype multi-system seasonal forecast service is now available on the C3S website.

The initial release consists of deterministic and probabilistic forecasts for sea-surface, near-surface air and upper air (850 hPa) temperature, geopotential height (500 hPa), mean sea level pressure and precipitation. The forecasts provide seasonal (three-month) means and have a range of six months. They can be viewed both for the multi-system combination and the individual contributions (the comparison of the single-system forecasts can give an indication of uncertainty in the forecast). The products are released on the 15th day of each month. The product list offers links to maps or time series for the forecast variables and the facility to navigate to the full set of graphics.

Future updates to the product portfolio will add new variables, monthly-mean estimates and associated skill information, and new indices and forecast products (e.g. climagrams). A data service is also under development. It will allow users to download both the original data the graphical products are based on and post-processed data. More details on the implementation of the service and access to the initial-release products are available at <http://climate.copernicus.eu/seasonal-forecasts>.

C3S and EUROSIP

Readers familiar with EUROSIP, a multi-system seasonal forecast activity coordinated by ECMWF since 2005,

may wonder how these two activities relate to each other. While both aim to put into practice the multi-model approach, whose benefits have been explored in research projects like DEMETER and ENSEMBLES, their scope is rather different. C3S is aimed at a larger audience and has an open data policy. EUROSIP data, which is archived at ECMWF, can be accessed subject to the terms of the more restrictive EUROSIP data policy.

The partners involved are also different. The three core C3S providers are all partners in EUROSIP, but EUROSIP also includes NCEP (the US National Centers for Environmental Prediction) and JMA (Japan Meteorological Agency) as associated partners. At the same time, as described above, C3S actively supports the development and implementation into operations of new seasonal forecasting systems in two European centres. Their output will be included in the forecast products offered by the service.

As it stands, the two state-of-the-art forecasting systems from the associated partners in EUROSIP are absent from the C3S multi-system. At their next meeting, in early 2017, the EUROSIP steering group will discuss options for a transition to a well-resourced, operational C3S multi-system seasonal service.

Multi-decadal variability in predictive skill of the winter NAO

ANTJE WEISHEIMER (ECMWF and University of Oxford), **NATHALIE SCHALLER**, **CHRISTOPHER O'REILLY**, **DAVID MACLEOD**, **JAMES HEATLEY**, **TIM PALMER** (all University of Oxford)

Results obtained from a new long dataset of ensemble seasonal hindcasts show that there is substantial multi-decadal variability in the skill of predictions of the North Atlantic Oscillation (NAO). This variability appears to be correlated with features of the large-scale circulation including the state of the NAO itself, the El Niño–Southern Oscillation (ENSO) and the Pacific Decadal Oscillation (PDO). The NAO is an irregular oscillation in atmospheric flow patterns in the North Atlantic Ocean which has a strong influence on the weather and climate in Western Europe.

Understanding the seasonal predictability of circulation anomalies over the Euro-Atlantic region has long been and continues to be a challenge. Based on skill estimates from hindcasts made over the last couple of decades, recent studies have suggested that considerable success has been achieved in forecasting the NAO

during winter using current-generation dynamical forecast models. However, studies using previous-generation models had shown that forecasts of winter climate anomalies in the 1960s and 1970s were less successful than forecasts of the 1980s and 1990s. Given that the more recent decades have been dominated by the NAO in its positive phase, it is important to know whether the performance of current models would be similarly skilful when tested over periods marked by a predominantly negative NAO.

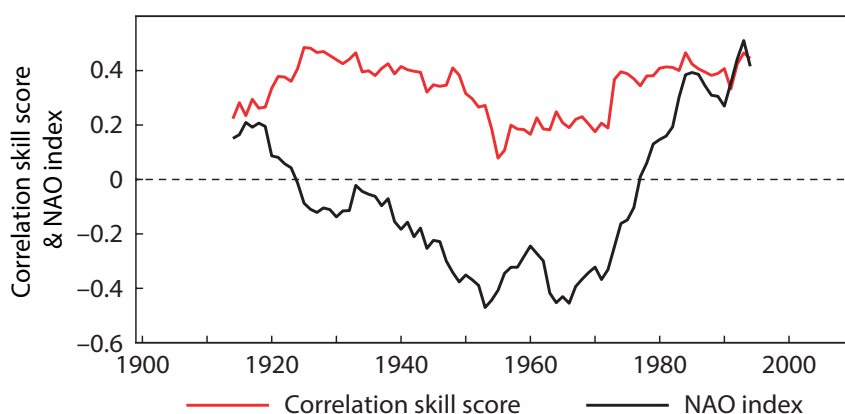
To this end, a new long dataset of ensemble seasonal hindcasts has been generated with the atmospheric part of ECMWF's Integrated Forecasting System (IFS). This data covers the period 1900 to 2010 and is named Atmospheric Seasonal Forecasts of the 20th Century (ASF-20C). The ASF-20C hindcasts were performed with IFS Cycle 41r1, using a similar horizontal and vertical resolution as ECMWF's currently operational seasonal forecasting System 4. The hindcasts were initialised with, and verified against, ECMWF's atmospheric reanalysis of the 20th century (ERA-20C) and use observed sea-surface temperature (SST) and sea-ice data at the lower boundary over the ocean.

The ensemble comprises 51 ensemble members. Although hindcasts were produced for all seasons, we focus here on the analysis of winter hindcasts (December–February, DJF), that is those initialised on each 1 November from 1900 to 2009. These new data provide a unique tool to explore many aspects of atmospheric seasonal climate prediction. The unprecedented length of the period covered allows for a thorough inspection of the robustness of seasonal forecast skill estimates and their variability on a timescale much longer than in previous studies.

Our findings are that the predictive skill of the NAO is non-stationary and has multi-decadal variability, with higher levels of skill during recent decades and in the early parts of the 20th century and lower levels of skill during the mid-century decades. Interestingly, the NAO index itself shows a somewhat similar behaviour, with negative values in an extended period around the middle of the century and positive amplitudes in recent decades and at the beginning of the century.

Interpreting the results

There is evidence for a meteorological explanation of such non-stationary predictability. We have assessed the extent to which the multi-decadal variability in skill co-varies with variations in the general circulation itself. While there is no obvious statistical reason why these two time series should be correlated, we find strong co-variations between time series of NAO skill and low-frequency time series of the NAO itself over the whole 20th century. For example, the mid-century decades of low correlation skill correspond with periods when the NAO was in a strongly negative phase. At first glance these results suggest that the model is struggling to predict the circulation in periods with negative NAO. However, it is not the case that in general the forecast model cannot skilfully predict negative NAO winters. Rather, our analysis suggests that probabilistic forecasts for strong negative and all ranges of positive NAO indices are



Correlation skill score and NAO index. Time series of the correlation skill score for the ensemble mean of hindcasts of the NAO for the months of December–February initialised on 1 November, computed for overlapping 30-year windows shifted by one year at a time and plotted at the 15th year of each window; and of 30-year running mean NAO index values for the months of December–February in ERA-20C. The interannual correlation skill score for predictions of the winter NAO index over the entire period from 1900 to 2010 is significantly positive ($r = 0.31$, with $r = 1$ indicating perfect correlation and $r = 0$ indicating no correlation).

highly skilful. Indeed, the model is remarkably good at predicting strong negative NAO winters. For example, the events associated with the highest ROC skill score are those below the 10th percentile of the climatological distribution. However, the model does not perform as well for weak negative NAO events. The overall skill in the first half of the 20th century stems from skilfully predicting a wide spectrum of NAO events.

To try to understand these results, we have studied correlations between NAO forecast skill and decadal timescale diagnostics of the general circulation further afield, such as ENSO and the PDO. The forecast skill for each of the 30-year periods does seem to be related to the dominant phase of El Niño, with periods of positive SST anomalies in the central tropical Pacific coinciding with periods of strong NAO skill in the hindcasts. This is also the case for the PDO,

which is in a positive phase during periods when the hindcasts are most skilful. These correlations with the general circulation suggest that the decadal variations in NAO forecast skill are indeed linked to the general circulation. More specifically, the NAO forecast skill seems to be correlated most strongly with variations in SSTs in the tropical Western Pacific and the Indian Ocean. Further numerical experiments are needed to understand such teleconnections.

As explained in greater detail in an article by the authors in the *Quarterly Journal of the Royal Meteorological Society* (doi:10.1002/qj.2976), during the mid-century period of low skill the DJF NAO exhibits remarkable persistence from the November NAO. It is further found that the decades of high NAO persistence from the 1940s to the 1970s coincide with periods of enhanced intra-seasonal variability of geopotential height at 500 hPa over

the Atlantic sector. These findings are consistent with the hypothesis that upper-level Rossby wave-breaking events occur more frequently during periods of negative NAO than during periods of positive NAO, which will be a focus of future research.

In conclusion, the mid-century decades stand out as an important period on which to test the performance of future seasonal forecast systems. Achieving good forecast skill for the more recent decades with predominantly positive NAO indices is not sufficient to guarantee similarly good performance for decadal periods with negative NAO index, which might occur again in the future. Our findings underline the importance of a representative re-forecast dataset for robust conclusions about the levels of predictive skill in predicting the Atlantic-European climate in the future.

ECMWF meets Ibero-American weather services

XAVIER ABELLAN

ECMWF was kindly invited to attend the 13th CIMHET meeting (Conference of the Directors of Ibero-American Meteorological and Hydrological Services), which took place in Antigua, Guatemala, from 23 to 25 November. The event was organised and coordinated by Spain's meteorological agency, AEMET, and held in Spanish. Every one and a half years it brings together the Directors and delegates from 20 Ibero-American national meteorological and hydrological services (NMHS).

Our mission was to present and raise awareness of ECMWF products and licences available to them as World Meteorological Organization NMHS, as well as outlining ECMWF's new Strategy 2016–2025. The presentation was very well received. Many countries were impressed by the web and eCharts products and showed an interest in having access to the data.

As part of the visit, we provided a demonstration account for the web



Opening session. The meeting brought together Directors and delegates from 20 Ibero-American national meteorological and hydrological services.

NMHS non-commercial licence. This was also highly appreciated and prompted positive feedback. Colombia and Mexico, the two countries already holding a full WMO NMHS licence, expressed their satisfaction with the quality of the products they receive

and recognised that they play a key role in their forecasts.

The meeting was structured around three main topics:

- Training
- Institutional development and resource allocation

- Meteorological, hydrological and climatological service delivery

The forum started back in 2003 to increase the cooperation and coordination among NMHS in the region and to build a closer community among countries that share more than just the language, face the same challenges and have similar needs.

The conference took place at the Training Centre of the Spanish Cooperation in Antigua, an old school

founded in 1608 by the Jesuits. Over the years it has had many uses, including as a fabric factory and a market. Following substantial refurbishment, it now hosts one of the four training centres that the Spanish Agency for International Development Cooperation (AECID) has in the Latin American region.

As chance would have it, a small earthquake interrupted my presentation for a minute! Thankfully

no evacuation was needed because Antigua was far away from the epicentre and just experienced a small tremor.

Overall, the participants were pleased that someone from ECMWF had attended the meeting and contributed to it, as was formally acknowledged in the Declaration of the 13th CIMHET Meeting. More information about the conference can be found at <http://cimhet.org> (in Spanish).

Experts debate future of supercomputing in meteorology

SAMI SAARINEN

The 17th Workshop on High Performance Computing in Meteorology took place at ECMWF from 24 to 28 October 2016. The theme of this biennially organised workshop was the scalability of numerical weather prediction (NWP) systems. Over the four and a half days, more than 40 speakers presented their vision of what kind of systems and programming paradigms we might be using in a few years' time or even in the next decade. The event was attended by 100 external participants from ECMWF's Member and Co-operating States as well as from the USA, Canada, Japan, South Korea and Australia. Computer vendors and software providers were also present.

Keynote talks were given by Dr Jack Dongarra from the University of Tennessee, who developed the LINPACK test used to estimate the performance of supercomputers, and by Dr Thomas Schulthess, the Director of the Swiss National Supercomputing Centre (CSCS), who has been in charge of installing the largest GPU-cluster in Europe for operational weather prediction. Dr Dongarra gave an update on the latest HPC developments and set out the 'changing rules at exascale', while Dr Schulthess asked whether exascale computing represented the 'endgame' or a 'new beginning for climate modelling'. In addition, a talk by Professor Tim Palmer from the University of Oxford on using lower precision in meteorology triggered a lot of discussion.

The decision to distribute and mix the talks across the week paid off as this kept the momentum going and there were no sessions without interesting topics. We also introduced a new kind of panel discussion, which took place on Thursday afternoon and gave rise to a lot of debate and exchanges of ideas on how to develop NWP coding to make it fit for future systems.

The presentations and video recordings of the talks are available online at www.ecmwf.int/en/learning/workshops-and-seminars/17th-workshop-high-performance-computing-meteorology. The next HPC workshop will take place in the autumn of 2018.



Workshop participants. The 17th Workshop on High Performance Computing in Meteorology was attended by 100 external participants from ECMWF's Member and Co-operating States, the USA, Canada, Japan, South Korea and Australia.

New IFS cycle brings sea-ice coupling and higher ocean resolution

ROBERTO BUIZZA, JEAN-RAYMOND BIDLOT,
MARTIN JANOUSEK, SARAH KEELEY,
KRISTIAN MOGENSEN, DAVID RICHARDSON

On 22 November 2016, ECMWF implemented a new version of its Integrated Forecasting System (IFS Cycle 43r1), which for the first time includes an interactive sea-ice model in the medium-range/monthly ensemble forecast (ENS). Other key features include a four times finer horizontal resolution in the ocean model and the use of a new, higher-resolution ocean ensemble of analyses and reanalyses, ORAS5. IFS Cycle 43r1 also brings changes in the use of observations, data assimilation and modelling, and it introduces a range of new parameters. The various changes and upgrades have led to significant improvements in forecast quality.

Dynamic sea ice

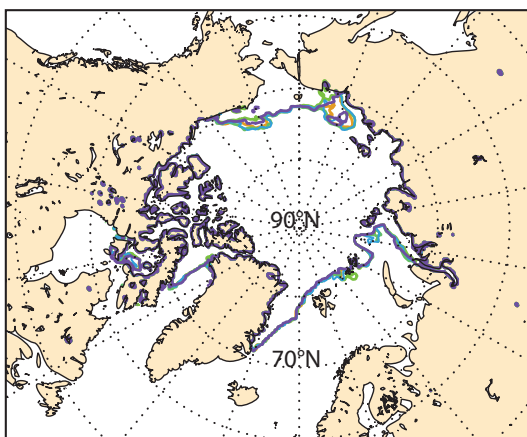
The interactive sea-ice model LIM2, the Louvain-la-Neuve Sea Ice Model developed at the Belgian Université catholique de Louvain, has been implemented, allowing sea-ice cover to respond to changes in the atmosphere and ocean states. This allows, for example, for the melting of sea ice in ENS during atmospheric warming in spring, and in general it enables a more accurate interaction between sea ice, ocean and atmosphere. LIM2 is part of the NEMO (Nucleus for European Modelling of the Ocean) modelling framework also used at ECMWF to model the ocean. The ENS ocean and sea-ice initial conditions are provided by the new ocean analysis and reanalysis ensemble (ORAS5), which uses the new ocean model described below and a revised ensemble perturbation method. ORAS5 has been running in parallel to ORAS4 since August 2016 and covers the period 1975 to the present.

Figure 1 shows an example of the evolution of sea ice in the ENS. Figure 1a shows the five sea-ice initial conditions which are distributed across the 51 ensemble members to help initialise the ENS. The five initial conditions are generated by the new ORAS5 ensemble of ocean analyses. Figure 1b shows 23-day forecasts and the corresponding control (ORAS5 member-0) analysis. The figure shows that the sea-ice edge evolves in the forecast, expanding to cover a larger area. It also shows that there is a degree of uncertainty in the prediction, with some areas characterised by a larger spread among the 51 forecasts. Finally, it shows that the verifying analysis is almost everywhere included in the range spanned by the ensemble.

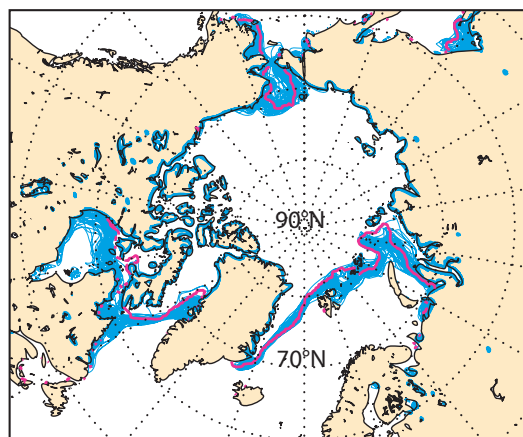
Higher ocean resolution

With this cycle upgrade, the ENS sees a major upgrade in the NEMO consortium's ocean model: the resolution has been increased from 1 degree and 42 layers to 0.25 degrees and 75 layers, the ORCA025z75 ocean model configuration based on the configuration developed by the DRAKKAR group. The increase in vertical resolution is particularly large in the uppermost part of the ocean, with an increase in the number of levels in the first 50 metres from 5 to 18. The horizontal resolution increase means that small-scale ocean circulation features are better captured and coastlines and bathymetry are better resolved than previously, as shown in Figure 2. The vertical resolution increase means that the diurnal cycle of sea-surface temperatures (SST) is much better captured, with a 1-metre top level in the new configuration compared to the previous 10-metre top level. The SST continues to be partially coupled to the atmosphere for the first week. The ocean upgrade makes the ocean more responsive to changes in the atmospheric

a Initial conditions



b Forecast and analysis



— Forecast — Analysis

Figure 1 Forecasts and analyses of sea-ice edge, showing (a) the five analyses of the ORAS5 ensemble of analyses, used to initialise the ECMWF medium-range/monthly ensemble on 7 November 2016 at 00 UTC and (b) the 51 ENS 23-day forecasts for the sea-ice edge on 30 November 2016 and the corresponding sea-ice analysis.

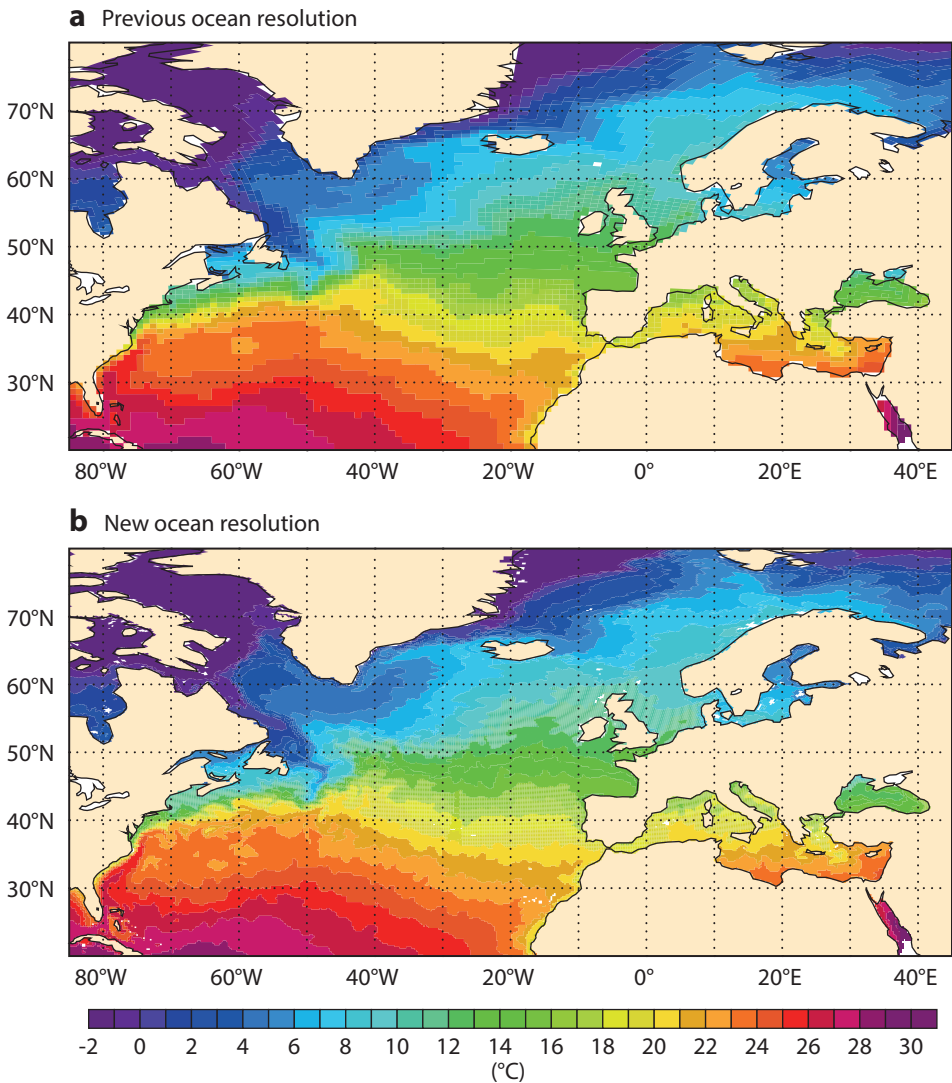


Figure 2 The higher ocean resolution for ensemble forecasts in IFS Cycle 43r1 results in forecast fields that reveal more detailed features and fit more snugly along coastlines. This is illustrated by these forecasts of daily mean sea-surface temperature for 18 November 2016, initialised at 00 UTC on the same day, using (a) the previous model version and (b) the new model version.

state and leads to a larger ensemble spread due to more variability in the ocean.

Other changes

Cycle 43r1 includes changes in the use of observations, data assimilation and in modelling, based on the results of research carried out at the Centre.

In data assimilation, for example, the method used to perturb the sea-surface temperature in the Ensemble of Data Assimilations (EDA) has been improved, and a higher-resolution EDA-based estimate of background errors (from TL159 to TL399 resolution) has been introduced. Furthermore, in the high-resolution assimilation, a weak-constraint method has been activated in the stratosphere (above 40 hPa). In terms of observations, 43r1 includes a new slant-path radiative transfer for all clear-sky sounder radiances used when interpolating model fields to observation locations. It also includes updated observation error covariance matrices and a change in the ozone anchor channels for IASI (Infrared Atmospheric Sounding Interferometer) and CrIS (Cross-track Infrared Sounder), obtained through a better treatment of observation

uncertainty, and a new aerosol detection scheme for IASI, CrIS and AIRS (Atmospheric Infrared Sounder).

In modelling, 43r1 includes changes in boundary layer cloud for marine stratocumulus, and the use of a new ozone climatology. The land surface coupling coefficients for forest tiles have been modified to reduce night-time 2-metre temperature errors and improve the diurnal cycle. To improve the interactions between turbulent mixing (vertical diffusion), shallow convection and cloud parametrizations relevant to boundary layer cloud, changes have been introduced to the mass flux limiter, the up-draught momentum and the environment for shallow convection. These changes lead to increased cloud cover in the maritime subtropical stratocumulus decks, reducing forecast errors. The stochastic model error scheme SPPT (Stochastically Perturbed Parameterized Tendencies), which is active in both the EDA and the ENS perturbed members, has been revised, with the introduction of tendency mass conservation constraints.

New parameters

There are five new cloud and temperature diagnostic

parameters in IFS Cycle 43r1 and improvements to others, as requested by users. The new parameters are (in brackets: grib identifier, short name and units):

- Ceiling: cloud base height relative to the ground (260109, ceil, m)
- Height of convective cloud top (228046, hcct, m)
- Height of zero degree wet bulb temperature (228047, hwbt0, m)
- Height of one degree wet bulb temperature (228048, hwbt1, m)
- Direct solar radiation, incident on a plane perpendicular to the sun's direction (47, dsrp, J/m⁻²)

Furthermore, eight new wave model output fields are generated:

- The magnitude and direction of the wave energy flux that is responsible for the impact of the waves on coastlines and offshore structures;
- Significant wave height of all waves in six different period ranges to help with the detection of low-frequency wave energy (Figure 3).

Better forecasts

Comparison of scores with the previous operational cycle 41r2 indicates that, for upper air fields, the new model cycle provides improved high-resolution forecasts (HRES) and ensemble forecasts throughout the troposphere and lower stratosphere (Figure 4). In the extratropics, error reductions of the order of 0.5-1% are found for most upper-air parameters and levels.

Improvements are most consistently seen in verification against the model analysis. In the tropics, there is a small degradation (both against analysis and observations) of temperature near the tropopause in terms of root-mean-square error (RMSE) but not in terms of anomaly correlation. This is due to a slight cooling caused by a modification in the treatment of cloud effects in the vertical diffusion scheme, which overall leads to improved cloud cover. While there is a consistent gain for upper-air parameters on the hemispheric scale, some continental-scale areas, such as North America and East Asia, show statistically significant improvements only at some levels and for some parameters.

Increases in upper-air skill of the ENS are generally similar to the single high-resolution forecast, with a substantial gain for mean sea level pressure. The improvement in the primary headline score for the ENS is small: a gain of about 0.5 hours in the skilful range of ensemble forecasts of 850 hPa temperature in the extratropical northern hemisphere, defined as the lead time at which the Continuous Ranked Probability Skill Score drops below 25%. The spread-error relationship is generally improved, partly due to reduced error and partly due to increased spread. For some parameters this improvement is quite significant, such as 850 hPa wind speed in the tropics, where underdispersion is reduced by about 20% in the medium range.

In terms of weather parameters and waves, IFS Cycle 43r1 yields consistent gains in forecast performance in the

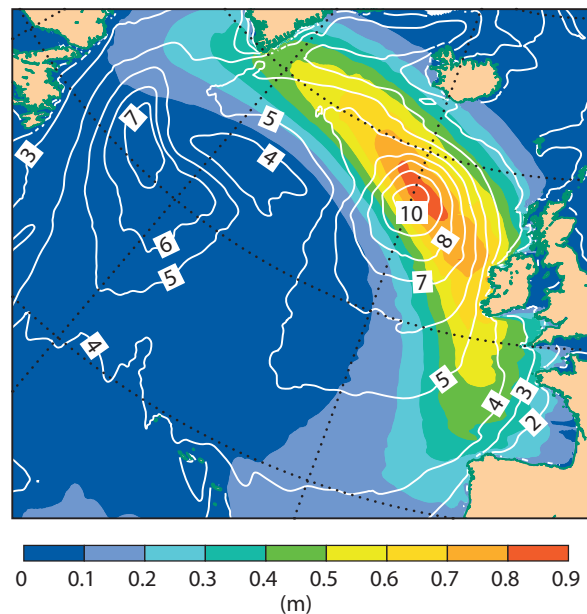


Figure 3 Seven-and-a-half-day (180-hour) forecast for significant wave height for all waves (contours) and for one of the new parameters, the significant wave height for all waves with periods between 21 and 25 seconds (shading), initialised at 00 UTC on 2 December 2016. Even though the highest significant wave heights are still confined to the storm location, in the Atlantic south of Iceland, long waves from that storm, as depicted by this new parameter, are already affecting coastlines from Iberia to South Greenland.

tropics and extratropics for total cloud cover, mostly due to a reduction of the negative bias in low cloud cover. Changes in precipitation over land areas are small and overall neutral. In the HRES, the increase in forecast skill for 2-metre temperature is most pronounced in the short and medium range, where it amounts to a reduction of about 1% in RMSE in the northern hemisphere extratropics, and of up to 2% over some land areas, such as Europe and North America. In the tropics there is an increase of 0.5–1% in the RMSE for 2-metre temperature, connected to a slight increase of the overall cold bias at low latitudes. In the ENS there is a significant improvement in 2-metre temperature amounting to a 3% reduction in the Continuous Ranked Probability Score (CRPS) in Europe. Ten-metre wind speed shows error reductions of 0.5–1% over the ocean, leading to improvements in significant wave height and mean wave period, especially in the tropics and the southern hemisphere. Over land areas, changes in 10-metre wind speed forecast skill are generally neutral to slightly positive.

For the monthly forecast range, results indicate a modest positive effect on skill scores although the differences are not statistically significant. There is a substantial improvement in the skill scores for the Madden-Julian Oscillation, corresponding to a gain in lead time of 0.5–1 day at a forecast range of 4 weeks. The MJO spread is increased, bringing it closer to the RMSE. Verification of precipitation against analysis shows some degradation in the tropics, which is not statistically significant, and a reduction of precipitation biases in the northwest Pacific.

Impact of orographic drag on forecast skill

IRINA SANDU (ECMWF), AYRTON ZADRA (Environment and Climate Change Canada), NILS WEDI (ECMWF)

The flow of the atmosphere is strongly influenced by various features on the Earth's surface: vegetation, buildings, hills, mountains, ice ridges or ocean waves all slow down or deflect the airflow in a variety of ways. Close to the surface, the air is slowed by friction and deflected by larger obstacles, such as mountains. Atmospheric gravity waves triggered by mountains propagate upward and slow down the flow where they break, generally in the upper troposphere and in the stratosphere. All these processes contribute to the drag exerted by the Earth's surface on the atmosphere.

The drag exerted by topography (orographic drag) plays an important role for many aspects of the large-scale circulation, such as the northern hemisphere winter extratropical circulation, including the position of storm tracks in the North Atlantic. However, the representation of orographic drag processes in models is particularly challenging. First, the resolution of most global climate and numerical weather prediction (NWP) models is not fine enough to represent in the required detail surface features such as hills or mountains and the disturbances they introduce into the airflow. A model can only directly capture the effects of mountains that are several times larger than the model grid spacing (the mean or resolved orography, Box A). The effects of disturbances induced by smaller mountains (subgrid or unresolved orography) have to be parametrized (Box B). Furthermore, it is impossible to directly measure the amount and distribution of drag globally, or even regionally. In the absence of observational constraints, the parametrizations

of these effects rely on heavily simplified assumptions mostly based on linear theory and idealized mountains. The extent to which they capture the non-linear effects exerted by complex topography remains unknown. As a result, the representation of orographic drag processes remains one of the major sources of uncertainty in NWP and climate models.

Here we show that the representation of the mean orography differs even among models with similar resolution. We also illustrate how much models differ in terms of subgrid surface stress (or friction) and its partition among various processes. Finally, we use ECMWF's Integrated Forecasting System (IFS) to demonstrate that these issues significantly affect forecast skill.

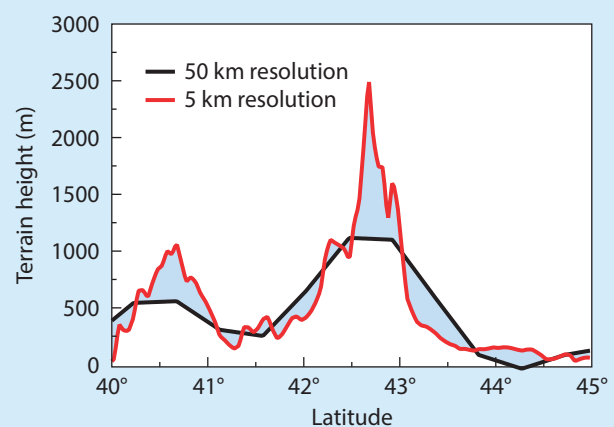
Differences in orography

The mean orography used by global NWP models can be compared in terms of its variance at different scales (Figure 1). It appears that even models with a similar resolution differ significantly in terms of the orographic variance at the highest wavenumbers (smallest scales). For example, the Canadian Meteorological Centre's Global Deterministic Prediction System (GDPS) and the UK Met Office's Unified Model (UM) have much less variance at the smallest scales than IFS TL799, which is indicative of a smoother mean orography. The same is true when comparing the German National Meteorological Service's ICON model with IFS TCo1279. This may seem surprising as one would expect models with a similar resolution to have similar orographies.

However, in practice, especially at the smallest scales, the orographic variance crucially depends on any filtering of the

Mean and subgrid orography

The mean or resolved orography is the orography that is directly taken into account in the basic equations describing the flow. It is representative of mountains with scales equal to or larger than the model horizontal resolution (or grid spacing). To derive it, at ECMWF a global 1 km resolution surface elevation dataset based on satellite observations is used to compute the mean elevation for each model grid box. The subgrid or unresolved orography represents mountains with scales smaller than the model horizontal resolution. For each target resolution, the differences between a reference orography and the mean orography are used to derive the characteristics of the subgrid orography. The reference orography is obtained from the 1 km resolution dataset by filtering out scales below 5 km. The standard deviation, slope, orientation and anisotropy of the subgrid orography then feed into the subgrid orography parametrization (Box B), which represents the drag exerted by topographical features not resolved by the model. The derivation of the mean and subgrid orography at ECMWF is described in detail in Part IV, Chapter 11 of the IFS Documentation.



South–north cross section of terrain height across the Pyrenees at 0° longitude using a 50 km and a 5 km resolution orography. The difference is the subgrid orography that enters into the subgrid orography scheme (SGO).

original orography dataset used to derive the orography at the model resolution; the type of grid the model uses (linear, cubic, quadratic, icosahedral); and the degree of numerical diffusion applied. Moreover, in the past, dynamical cores were less performant than today and the orography has therefore often been smoothed in order to prevent model instability, unrealistic gravity waves and aliasing effects. The cubic octahedral grid used at present for high-resolution forecasts in the IFS (TCo1279) has only very little numerical diffusion and can stably support an orography with more variance in the small scales, thus providing a faithful representation of the original 1 km orography for almost all wavenumbers up to the truncation limit. It thus maintains much more orographic variance at the small scales than the other discretisations included in Figure 1.

Impact of orography

To what extent do differences in orography affect NWP skill? One way to answer this question is to examine how forecasts obtained with a certain NWP model change when the model is run with a different orography. We have used the IFS to perform several sets of ten-day forecasts using different orographies. The forecasts were run for a winter month when the circulation in the northern hemisphere is very sensitive to the representation of the orography. They were initialised every day at 00 UTC from the operational analysis for December 2015 and were run using a TL799 configuration that uses a linear grid and corresponds to a horizontal resolution of approximately 25 km at the equator.

The control set of forecasts was performed with the original TL799 mean and subgrid orographies (CTRL). In a first experiment (EXP1) the TL799 mean orography was replaced with a smoother mean orography, i.e. the orography corresponding to the TL255 configuration, which is used for the ERA-Interim reanalysis (corresponding to

Boundary layer and subgrid orography schemes

B

Models often use more than one scheme to represent the drag associated with subgrid surface features. The reason is that different schemes account for different surface-induced drag processes. In the IFS, the boundary layer scheme (BL) represents stress associated with unresolved elements of the Earth’s surface from horizontal scales of less than 5 km, while the subgrid orography scheme (SGO) represents stress associated with horizontal scales between 5 km and the model resolution. Each of these two schemes in turn accounts for several processes.

The boundary layer scheme uses a turbulence parametrization to represent turbulent drag associated with surface elements such as land use or vegetation. It also includes a turbulent orographic form drag parametrization (TOFD) to represent drag associated with subgrid orography elements at horizontal scales of less than 5 km, such as hills or individual mountains (*Beljaars et al., 2004*). Other models (e.g. the Unified Model of the UK Met Office) do not have a special parametrization for turbulent orographic form drag but represent it by artificially enhancing the surface roughness length over orography, so that the orographic form drag is implicitly represented by the turbulence parametrization.

The SGO scheme (*Lott & Miller, 1997*) also represents different types of drag: (i) low-level blocking (BLOCK), which occurs when the air lacks the energy needed to go over a mountain and is partially blocked and partially goes around the mountain instead; and (ii) gravity wave drag associated with the breaking of gravity waves caused by air parcels that are forced to ascend while moving over topographic features. The magnitude of these effects crucially depends on the characteristics of the subgrid orography, particularly the standard deviation of its elevation.

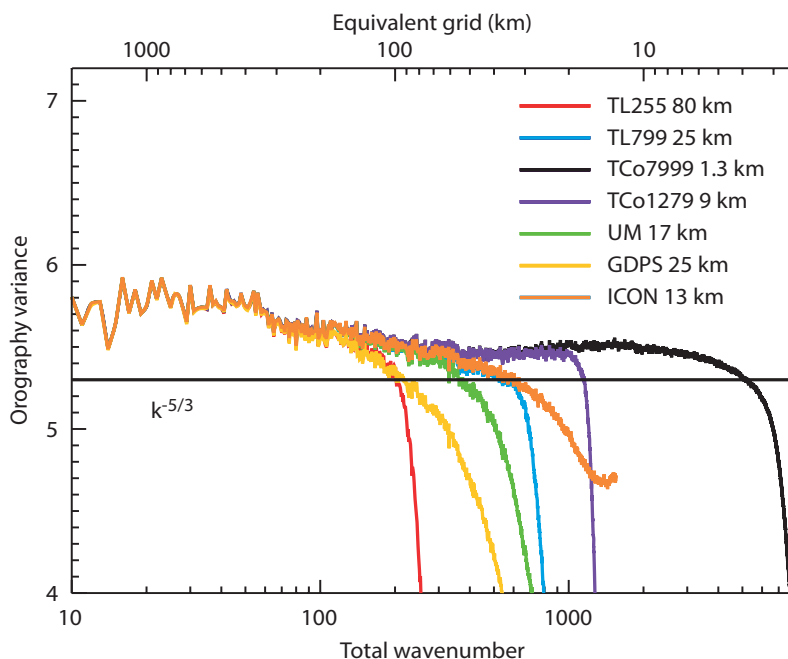


Figure 1 Variance of the mean orography scaled by the theoretical $k^{5/3}$ law (horizontal line) as a function of the total wavenumber for different cubic and linear discretisations in the IFS (TL255 – corresponding to the ERA-INTERIM reanalysis; TL799; TCo7999; and TCo1279 – corresponding to the operational high-resolution configuration) and in other global NWP models (the UK Met Office’s UM; the Canadian Meteorological Centre’s GDPS; the DWD’s ICON model).

approximately 80 km at the equator). The use of a smoother mean orography has to be accompanied by the use of a subgrid orography which accounts for the scales which are truncated out of the mean orography (in this case scales between wavenumbers 255 and 799). Therefore, in a second experiment (EXP2) both the TL255 mean orography and the subgrid orography fields corresponding to this smoother mean orography (derived by subtracting the TL255 orography from the 5 km dataset, see Box A) were used instead of the TL799 ones. These experiments aim to assess the impact of differences in orography similar to those found between the TL799 configuration and the GDPS model, which are run at the same horizontal resolution (Figure 1). Like the orography of the GDPS model, the TL255 orography contains much less variance at small scales than the TL799 orography.

EXP1 and EXP2 lead to a considerable deterioration in the representation of both near-surface variables and upper-air atmospheric variables throughout the forecast range compared to CTRL, as indicated by the increase in standard deviation (random error) in forecasts of 2 m temperature and geopotential height at 500 and 100 hPa in the northern hemisphere (Figure 2). The deterioration in 2 m temperature forecasts amounts to approximately 10% in the medium range and it is nearly entirely due to the use of a smoother mean orography (EXP1). There is also an increase in the absolute mean bias ranging from 0.5 to 3 K (after 24 hours) in all mountainous regions (not shown).

Computing the subgrid orography fields in a consistent way with the mean orography in EXP2 reduces the degradation in forecast skill seen in EXP1 in the upper troposphere, but it has virtually no effect near the surface (Figure 2c). A significant albeit smaller deterioration in forecast skill is also found for the southern hemisphere throughout the atmosphere. This is again related primarily to the change in mean orography (not shown). Similar results were obtained in experiments performed with the GDPS at a nominal resolution of 25 km, where the removal (or reduction) of the smoothing in the mean orography was shown to reduce the root mean square error (against radiosonde observations) of geopotential height at 500 hPa by approximately 2% in medium-range forecasts over the northern extratropics in winter (not shown).

The representation of the mean orography thus appears to play an important role for the prediction of both near-surface temperatures and large-scale circulation. This is not surprising since the low-level atmospheric spectra closely follow the mean orography spectra (not shown). The degradation in forecast skill resulting from using a smoother mean orography can only partially be alleviated by using more variability in the subgrid orography. This suggests that the parametrized drag does not affect the flow in exactly the same way as the resolved drag.

Differences in parametrized surface stress

The Working Group for Numerical Experimentation (WGNE) of the World Meteorological Organization (WMO) recently compared the parametrizations associated with surface

drag, i.e. the schemes currently employed by NWP and climate models to compute subgrid surface stresses (Zadra, 2013). This represented a first step towards a broader goal, namely to draw the attention of the scientific community to the importance of, and the challenges in correctly representing, momentum transfer in global models.

First results of this project suggest that while the inter-model spread is relatively small over the oceans, the total subgrid or parametrized surface stress is highly model-dependent over land (Figure 3). As the subgrid stress characterises the unresolved part of the flow, the inter-model spread found over land is in part due to differences in horizontal resolution. Nevertheless, the zonally averaged magnitude of the total subgrid stress can still differ by as much as 20% over land even for models of comparable resolution, such as the IFS and the UM (16 and 25 km at the time of the inter-comparison, respectively). These

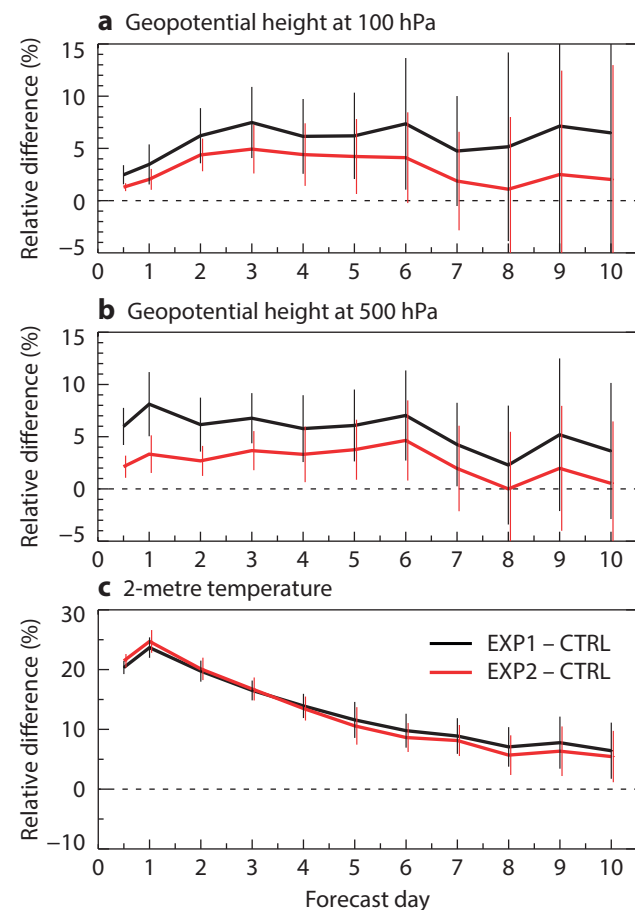


Figure 2 Relative difference in standard deviation (random error) between EXP1 and CTRL and between EXP2 and CTRL for forecasts of (a) geopotential height at 100 hPa, (b) geopotential height at 500 hPa, and (c) 2-metre temperature for the northern hemisphere extratropics (20°–90°N) in December 2015. A positive difference indicates a deterioration of the model performance in the experiment with respect to the CTRL. When error bars are entirely above/below the zero line, the performance of the respective experiment is significantly worse/better (95% confidence interval) than the CTRL. For all experiments the standard deviation was computed with respect to the corresponding analysis.

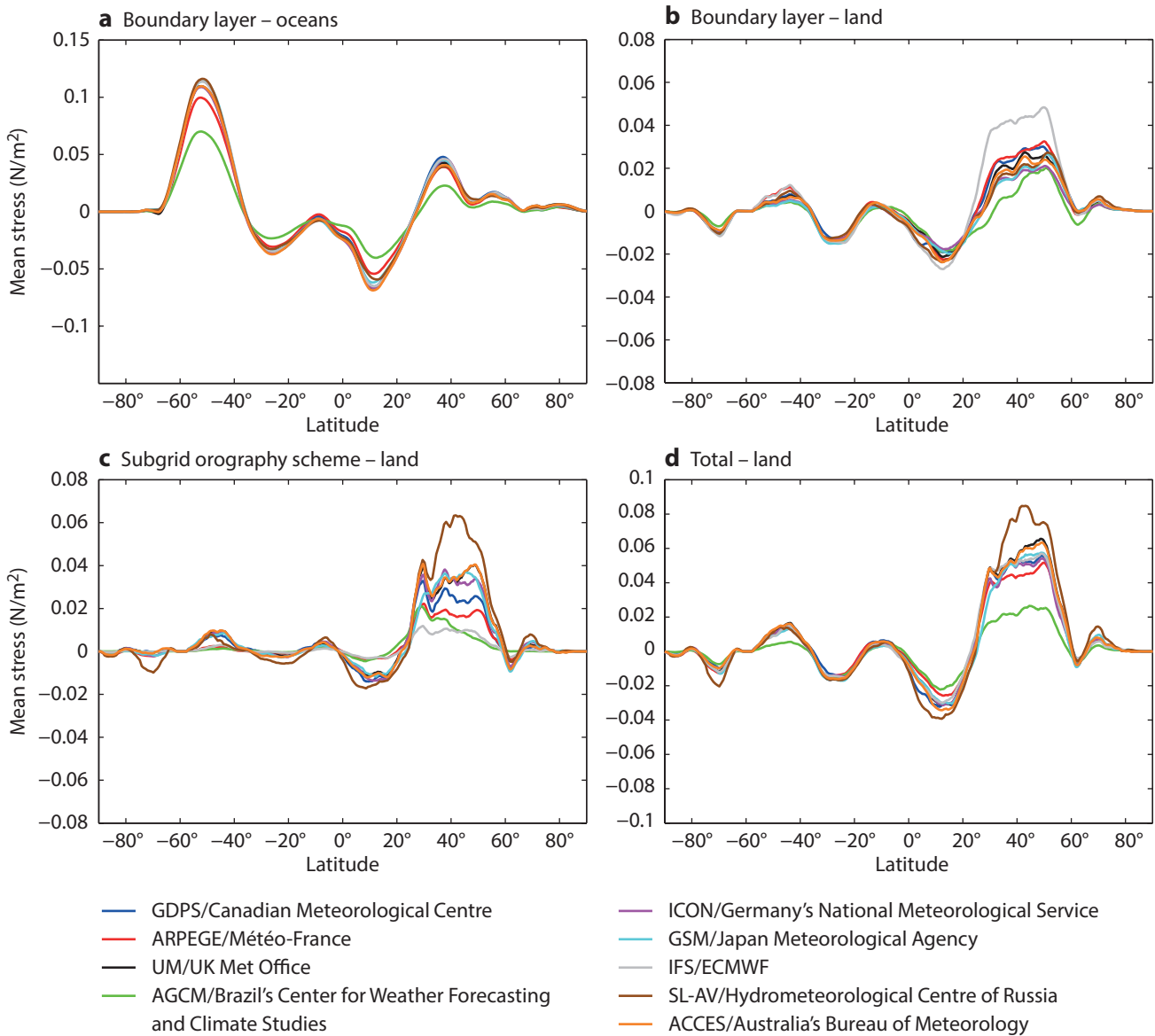


Figure 3 Zonal averages of subgrid surface stress, using the 00–24 UTC average from the results submitted by the different groups to the WGNE Drag Project for short-range forecasts for January 2012, showing (a) the boundary layer contribution over oceans, (b) the boundary layer contribution over land, (c) the subgrid orography scheme contribution over land, and (d) the total subgrid surface stress over land.

differences in the zonal average stress are mostly related to differences in stress over orography (not shown). Moreover, the partitioning of the total stress between the boundary layer and subgrid orography schemes is also model dependent (Figure 3). The UM for example has almost twice as much subgrid orography stress and up to 50% less boundary layer stress than the IFS over land in the northern hemisphere. Finally, the diurnal cycle of the total stress is quite different among the models. Figure 4 shows that over the Himalayan region the UM has more stress than the IFS between 12 and 18 UTC but generally less stress between 00 and 06 UTC.

These differences have multiple reasons: the underlying subgrid orography fields are different; models use different schemes; the schemes are implemented in different ways;

they represent the dependency of stress on wind speed and stability in different ways; and there are a number of poorly constrained parameters entering the schemes that are often tuned to maximise NWP skill.

Impact of subgrid orography

The WGNE Drag Project emphasised the importance of further constraining the representation of subgrid stress in models, especially in regions with orography. It also highlighted the need to better understand to what extent the inter-model differences in subgrid stress affect the quality of forecasts or climate predictions. Here we illustrate how such inter-model differences in subgrid stress in regions with orography impact short- to medium-range forecasts.

Following the approach adopted by Sandu *et al.* (2016), differences in the total zonally averaged subgrid surface stress (over land areas) that resemble those found in the WGNE Drag Project were mimicked in the IFS by making changes that lead to an increase of the total subgrid surface stress over orography. One way to increase the subgrid surface stress over orography is to change the orographic drag parametrizations themselves, another is to change the underlying subgrid orography fields.

Several sets of ten-day forecasts were run for December 2015, with a TCo399 configuration (25 km at the equator, a possible future configuration for monthly and seasonal forecasts at ECMWF) with the following changes that all lead to an increased subgrid surface stress over orography: (a) a change in the BLOCK parametrization that leads to increased blocking from large mountains (BLOCK), (b) a change in the TOFD parametrization that leads to an increased form drag from hills (TOFD), (c) a change in the way the subgrid orography is computed (two sets of runs hereafter referred to as 4dx and 8dx). All runs lead to an increase of 5–15% in the zonally averaged subgrid surface stress over land in the NH with respect to a control (CTRL) run performed with the default model configuration.

The last set of runs were motivated by a recent study by Vosper *et al.* (2016), which suggested that the subgrid orography should not represent scales smaller than the grid box (or the headline resolution), but scales smaller than the effective resolution of the model. Indeed, due to the nature of numerical solutions and parametrizations, the effective resolution of a model is not equal to its headline resolution or grid box size but corresponds to a few grid spacings (4 to 8 dx depending on the model, where dx denotes the headline resolution). One can argue that the resolved orographic drag accounts only for scales larger than this effective resolution, and therefore

the subgrid or unresolved part should account for scales smaller than the effective resolution rather than the headline resolution.

To evaluate the impact of this hypothesis on forecast skill, the subgrid orography fields were recomputed for the 4dx and 8dx runs by taking the difference between the 5 km dataset (BOX A) and a mean orography smoothed by applying a 4dx and an 8dx filter respectively, instead of the dx filter used in the control run (CTRL). This approach generally leads to an increased standard deviation of the subgrid orography, and hence to an increased contribution to the total surface stress from the subgrid orography parametrization. In the 8dx experiment, for example, the standard deviation of the subgrid orography increases by a factor of two with respect to the CTRL run in the global average, but this factor exhibits strong local variations. The choice of these filters is motivated by the fact that the effective resolution for the cubic octahedral discretisation is about 4dx.

The enhancement in total subgrid surface stress simulated by increasing either the TOFD or the BLOCK stress, or by changing the underlying subgrid orography, leads to changes in the predicted mean surface pressure in a matter of hours (Figure 5). Thus, pressure gradient changes across the regions with the largest mountain chains (the Himalayas and the Rocky Mountains), as well as an increase in surface pressure over Europe, can already be observed within the first six hours of the forecasts (not shown). During the first 24 hours, these changes amplify and extend to larger spatial scales in all cases, although they have different strengths for the various experiments (Figure 5). As suggested by Zadra *et al.* (2003) and discussed in Sandu *et al.* (2016), the local response in surface pressure over the largest mountain chains can be understood in terms of geostrophic balance. The enhanced stress over orography

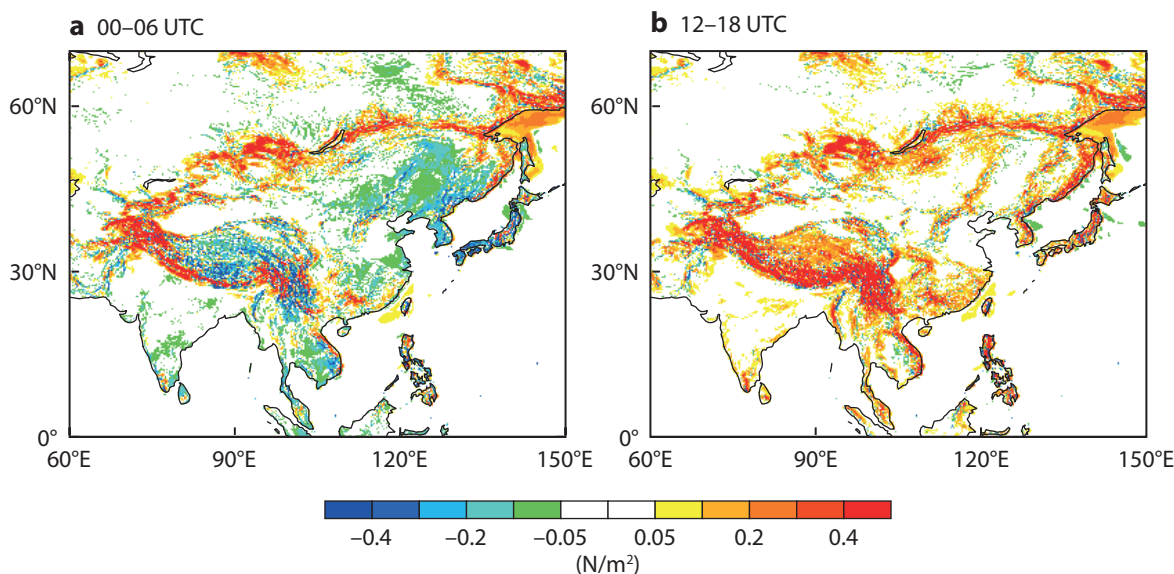


Figure 4 Difference in total surface subgrid stress between the UK Met Office’s Unified Model (UM) and the IFS for (a) 00–06 UTC and (b) 12–18 UTC, from the results submitted to the WGNE Drag Project for January 2012.

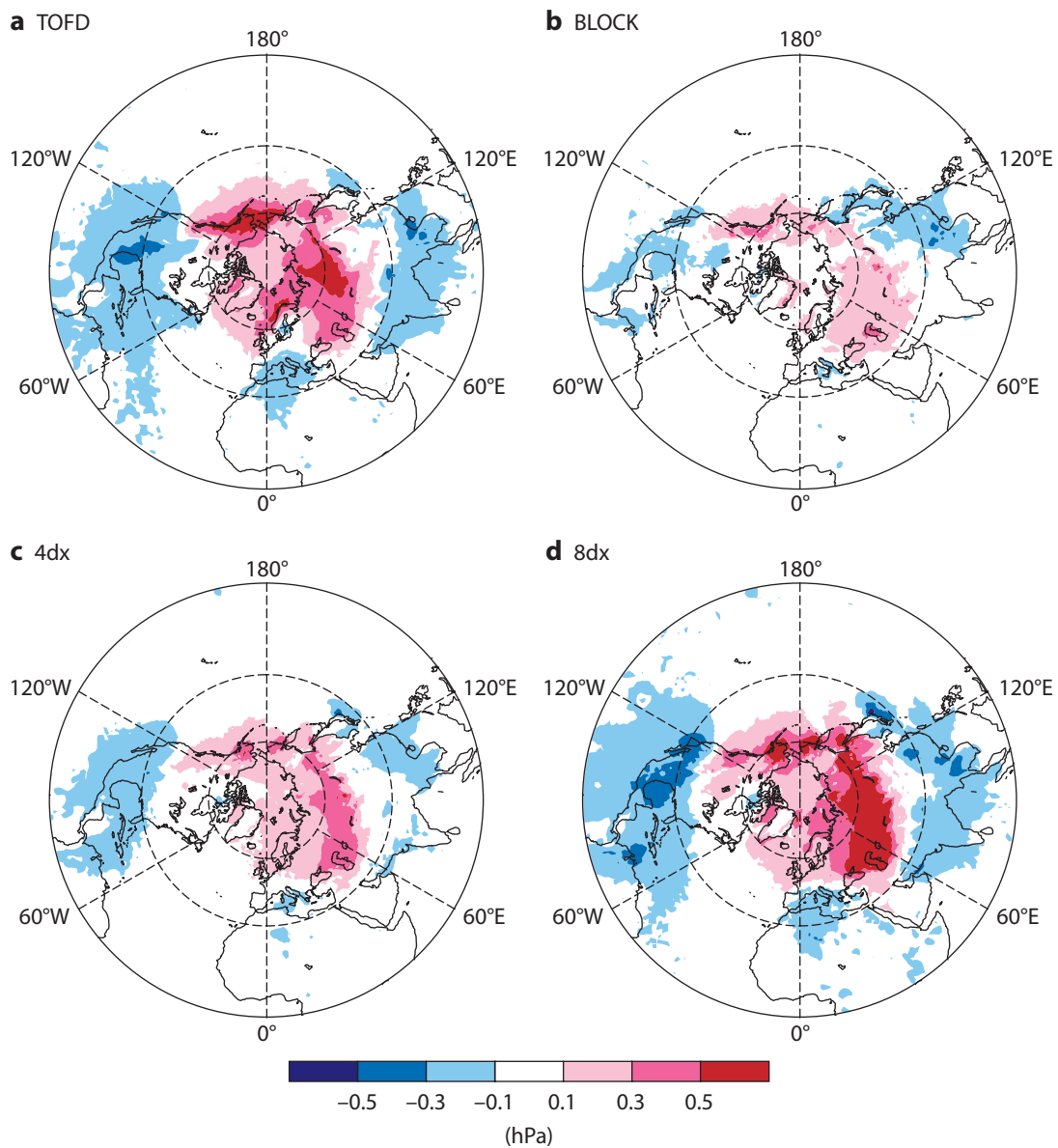


Figure 5 Mean change in surface pressure with respect to the CTRL run in the experiments in which (a) the TOFD stress is enhanced, (b) the BLOCK stress is enhanced, (c) the subgrid orography fields are computed using a 4dx filter, and (d) the subgrid orography fields are computed using an 8dx filter. The monthly means are based on 24-hour forecasts initialised at 00 UTC every day in December 2015.

slows down mid-latitude surface westerlies, which results in a meridional pressure gradient across the Rockies, the Alps and the Himalayas.

Although they are similar in terms of zonally averaged surface stress (within 10% over land), the different experiments have different impacts on forecast skill in the northern hemisphere (Figure 6). The changes to the TOFD stress considerably degrade the ability of the model to reproduce the hemispheric circulation in the entire troposphere up to forecast day 4, while those made to the BLOCK stress lead to a slight improvement of forecast skill at 500 hPa. The experiments with changed subgrid orographies also affect the large-scale circulation in different ways. The 4dx experiment seems fairly neutral on average over the hemisphere but has positive effects locally

(over North America and Asia, not shown), while the 8dx experiment significantly degrades the representation of the circulation up to forecast day 4.

These results illustrate that poorly constrained parametrizations and uncertainties in how best to construct the subgrid orography can translate into significant impacts on forecast skill.

Way forward

A lot of questions regarding orographic drag processes, their effects on the large-scale circulation and their representation in models remain open. For example, we need to better understand how orographic drag depends on thermal stability and wind speed and how surface orographic drag affects the flow on different timescales.

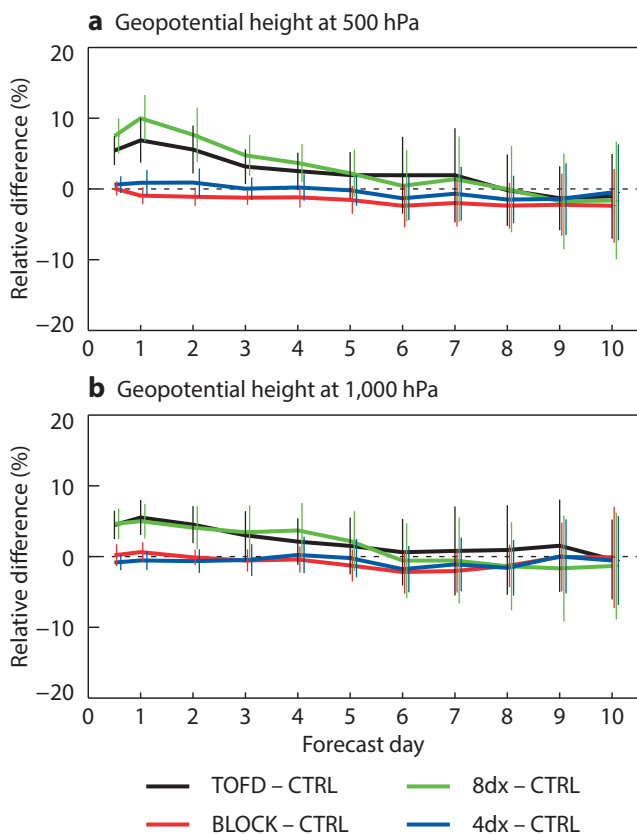


Figure 6 Relative difference in standard deviation (random error) between each of the experiments (TOFD, BLOCK, 4dx and 8dx) and CTRL for forecasts of (a) geopotential height at 500 hPa and (b) geopotential height at 1,000 hPa for the northern hemisphere extratropics (20°–90°N) in December 2015. A positive difference indicates a deterioration of the model performance in the experiment with respect to the CTRL. When error bars are entirely above/below the zero line the performance of the respective experiment is significantly worse/better (95% confidence interval) than the CTRL. For all experiments the standard deviation was computed with respect to the corresponding analysis.

FURTHER READING

Beljaars, A., A. Brown, & N. Wood, 2004: A new parameterization of turbulent orographic form drag, *Q. J. R. Meteorol. Soc.*, **130**, 1327–1347.

Lott, F., & M. Miller, 1997: A new subgrid orographic drag parameterization: Its formulation and testing, *Q. J. R. Meteorol. Soc.*, **123**, 101–127.

Sandu, I., P. Bechtold, A. Beljaars, A. Bozzo, F. Pithan, T.G. Shepherd & A. Zadra, 2016: Impacts of parameterized orographic drag on the Northern Hemisphere winter circulation, *J. Adv. Model. Earth Syst.*, **8**, 196–211, doi:10.1002/2015MS000564.

On the modelling side, we do not know how orographic drag should be partitioned between various schemes; what scales the subgrid orography should represent; and even how different modelling centres construct their mean and subgrid orography fields.

A recent workshop that brought together experts from major NWP centres and academia at ECMWF concluded that progress needs to be made in three fields in particular: (i) a better theoretical understanding of drag processes and their impacts on the circulation; (ii) a better understanding of inter-model differences; and (iii) using high-resolution simulations and observations as well as new techniques to understand model errors and to constrain and improve the representation of orographic drag in models. For more details on the workshop, see *Sandu & Zadra (2016)*.

The next activities of the WGNE Drag Project will aim to achieve a better understanding of inter-model differences in surface stress and to find ways to improve the representation of orographic drag in models. They include a survey regarding the way the mean and subgrid orography are derived in NWP and climate models; numerical experiments which aim to better define the appropriate sub-grid scales for orographic fields as a function of the model's (effective) resolution; and a comparison of the tendencies given by the various parametrizations in regions of maximum uncertainty.

Sandu, I. & A. Zadra, 2016: Experts discuss role of drag processes in NWP and climate models, *ECMWF Newsletter No. 149*, 8–9.

Vosper, S.B., A.R. Brown & S. Webster, 2016: Orographic drag on islands in the NWP mountain grey zone, *Q.J.R. Meteorol. Soc.*, doi:10.1002/qj.2894.

Zadra, A., 2013: *WGNE Drag Project – An inter-model comparison of surface stresses*. Report No. 1.

Zadra, A., M. Roch, S. Laroche & M. Charron, 2003: The subgrid-scale orographic blocking parametrization of the GEM model, *Atmos. Ocean*, **41**, 155–170.

doi:10.21957/ffs36birj2

CERA-20C: An Earth system approach to climate reanalysis

PATRICK LALOYAUX,
ERIC DE BOISSÉSON, PER DAHLGREN

ECMWF has completed the production of a new global 20th-century reanalysis which aims to reconstruct the past weather and climate of the Earth system including the atmosphere, ocean, land, waves and sea ice. This coupled climate reanalysis, called CERA-20C, is part of the EU-funded ERA-CLIM2 project, which builds on the ERA-CLIM project. The latter produced ERA-20C, a 20th-century reanalysis for the atmosphere, land and waves only (*Poli et al., 2016*).

First results show that CERA-20C improves on the representation of atmosphere–ocean heat fluxes and of mean sea level pressure compared to previous reanalyses. At the same time, there are undesirable discontinuities in ocean heat content and an excessive accumulation of Arctic sea ice.

To account for errors in the observational record as well as model error, CERA-20C provides a ten-member ensemble of climate reconstructions. As expected, the spread of the ensemble decreases over time as the observational record improves. However, verification for the year 2005 suggests that the spread should be larger to give a better indication of the confidence we can have in the reanalysis data.

History of reanalysis at ECMWF

Since its creation in 1975, ECMWF has been a key player in the production of reanalyses, which provide a numerical description of the recent climate by combining models with observations. The initial focus was on producing atmospheric reanalyses covering the modern observing period, from 1979. The first of these, FGGE, was produced in the 1980s, followed by ERA-15, ERA-40 and ERA-Interim. The next reanalysis in this series, ERA5, is now in production after many years of research and a great deal of technical preparation (*Hersbach & Dee, 2016*). ECMWF is also producing ocean reanalyses. In 2016, the ORAS4 system was replaced by ORAS5, which incorporates the latest

improvements in ocean models, data assimilation methods and forcing fluxes.

The various reanalysis products have proven to be an important resource for weather and climate-related research as well as societal applications at large. Reanalyses also support numerical weather prediction since they can be used for the initialisation of reforecasts, the calibration of ensemble forecasts and model validation and verification. Reanalyses make it possible to study the inter-annual variability of forecast skill and to test new model versions on past severe weather cases. ERA-Interim and ORAS5 are the current operational reanalyses at ECMWF for the atmosphere and the ocean, respectively. They are created via an unchanging frozen data assimilation system and model, which ingest all available observations to provide the best state estimate over the target period.

Extending these reanalyses further back in time is a tremendous scientific challenge as the observing system is very sparse before the availability of satellite data from the 1970s onwards, and especially before the arrival of radiosonde measurements in the 1930s. To tackle the unavoidable issue of the ever-changing observational network, the ERA-CLIM project has developed a whitelisting approach to data selection for reanalyses covering the whole 20th century. Instead of assimilating the full observing system at any time, only observations with a good spatial and temporal coverage over the entire century are used. Modern data assimilation systems are able to faithfully reconstruct the large-scale tropospheric circulation from surface pressure observations only. The quality of such reconstructions does depend on the observation density and will never outperform a system using all sources of observations, including satellite and upper-air measurements. However, by using a more consistent observational network the whitelisting approach avoids artificial variability and spurious trends generated by the introduction of new instruments. This makes it possible to extend climate reconstructions further back in time to cover a period of 100 years or more with a focus on low-

Dataset	Period	Type	Ensemble	Atmosphere	Land	Waves	Ocean	Sea ice
ERA-Interim	1979-present	Full observing system		✓	✓	✓		
ORAS5	1975-present	Full observing system	✓				✓	✓
ERA-20C	1900-2010	Selected observing system		✓	✓	✓		
ORA-20C	1900-2010	Selected observing system	✓				✓	✓
CERA-20C	1901-2010	Selected observing system	✓	✓	✓	✓	✓	✓

Table 1 List of selected ECMWF reanalysis datasets showing the period covered, the observing system used and the different Earth system components included in the climate reconstruction.

frequency climate variability. The overall aim is to improve our ability to produce consistent reanalyses of the climate system, reaching back in time as far as possible given the available instrumental record.

In this context, ECMWF has produced the uncoupled atmospheric reanalysis ERA-20C, which covers the period January 1900 to December 2010. ERA-20C assimilates only conventional observations of surface pressure and marine wind, obtained from well-established climate data collections. Model forcings are specified from CMIP5 (Coupled Model Intercomparison Project Phase 5) recommendations to obtain an appropriate climate reconstruction. The atmospheric lower boundary conditions are prescribed using the UK Met Office Hadley Centre's HadISST2 monthly analysis product for sea-surface temperature and sea ice.

ERA-20C has delivered three-hourly products describing the spatial and temporal evolution of the atmosphere, land surface and waves. Following a similar approach, the ORA-20C reanalysis reconstructs the ocean and sea-ice state over the 20th century. Temperature and salinity profiles are assimilated into the ocean model, which is also constrained by fluxes from ERA-20C and a sea-surface temperature relaxation towards the HadISST2 product. Table 1 summarises the main features of some of the reanalyses produced at ECMWF.

For researchers wondering which reanalysis is the most appropriate for their project, it is important to understand the fundamental differences between the different types of reanalysis produced at ECMWF. Users interested in a temperature reference in the stratosphere for the assessment of a satellite in the 1980s might for example want to use ERA-Interim or ERA5, while users interested in precipitation anomaly trends in Europe over the last century may wish to opt for ERA-20C or CERA-20C.

ECMWF has also released a model-only integration of the 20th century, known as ERA-20CM, which includes no data assimilation. It is an ensemble of ten atmospheric model integrations which can be used to determine the systematic climate errors of the model.

CERA-20C – a new approach

ECMWF's Roadmap to 2025, which summarises the Centre's new ten-year Strategy, highlights that, "As forecasts progress towards coupled modelling, interactions between the different components need to be fully taken into account, not only during the forecast but also for the definition of the initial conditions of the forecasts."

In this context, the reanalysis capabilities developed in the ERA-CLIM project have been extended to the ocean and sea-ice components in the ERA-CLIM2 project. A new assimilation system (CERA) has been developed to simultaneously ingest atmospheric and ocean observations in the coupled Earth system model used for ECMWF's ensemble forecasts (Box A). This approach accounts for interactions between the atmosphere and the ocean during the assimilation process and has the potential to generate a more balanced and consistent Earth system climate reconstruction.

Description of the coupled assimilation system

A

The CERA system is based on a variational method with a common 24-hour assimilation window shared by the atmospheric and ocean components. The coupled model is introduced at the outer-loop level by coupling ECMWF's Integrated Forecasting System (IFS) for the atmosphere, land and waves to the NEMO model for the ocean and to the LIM2 model for sea ice (*Laloyaux & Dee, 2015*). This means that air–sea interactions are taken into account when observation misfits are computed and when the increments are applied to the initial condition. In this context, ocean observations can have a direct impact on the atmospheric analysis and, conversely, atmospheric observations can have an immediate impact on the analysed state of the ocean.

For the CERA-20C datasets, the resolution of the atmospheric model is set to TL159L91 (IFS version 41r2), which corresponds to a 1.125° horizontal grid (125 km) with 91 vertical levels going up to 0.1 hPa. The ocean model (NEMO version 3.4) uses the ORCA1 grid, which has approximately 1° horizontal resolution with meridional refinement at the equator. There are 42 vertical ocean levels with a first-layer thickness of 10 m.

A new version of the CERA system is under development based on the coupled model at higher resolution, which will include a quarter-of-a-degree ocean model. This new coupled assimilation system will be used to produce a short reanalysis over a recent period. It will assimilate all types of observations including upper air, satellite, wave, land surface and sea-ice measurements.

CERA-20C is the first ten-member ensemble of coupled climate reanalyses of the 20th century (production details are given in Box B). It is based on the CERA system, which assimilates only surface pressure and marine wind observations as well as ocean temperature and salinity profiles. The air–sea interface is relaxed towards the sea-surface temperature from the HadISST2 monthly product to avoid model drift while enabling the simulation of coupled processes. No data assimilation is performed in the land, wave and sea-ice components, but the use of the coupled model ensures a dynamically consistent Earth system estimate at any time.

Impact of ocean coupling

Heat fluxes

One of the benefits expected from a coupled assimilation system is a more consistent treatment of the air–sea interface. When decoupled, the ocean and atmospheric systems use boundary conditions that do not take into account ocean–atmosphere feedbacks.

In ERA-20C, the atmospheric lower boundary conditions come from the HadISST2 sea-surface temperature and sea-ice product, which does not contain any information about the ocean dynamics. In ORA-20C, the ocean is forced by the ERA-20C fields, which are fixed and cannot adjust

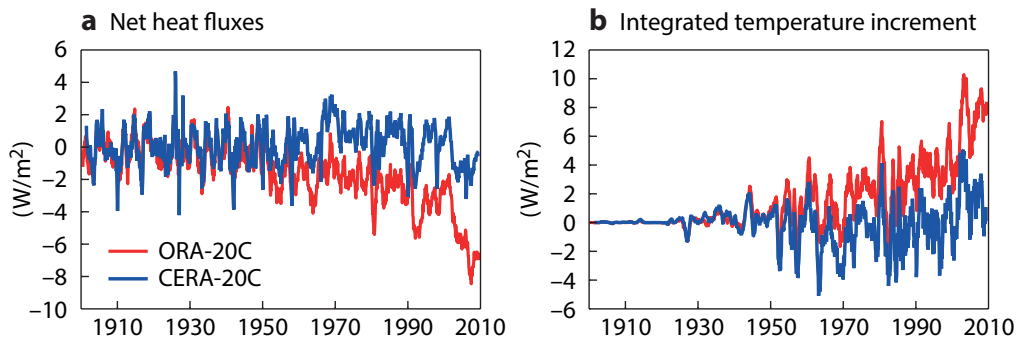


Figure 1 Time series of CERA-20C and ORA-20C control member values of (a) the global average of net air–sea heat fluxes and (b) the integrated temperature increment over the ocean.

to the ocean model behaviour. The long-term heat fluxes received by the ocean therefore suffer from inconsistencies at the air–sea interface. The resulting net heat fluxes over the ocean in ORA-20C show a negative trend from the 1940s onwards that tends to cool the ocean. To keep the ocean model close to the observed state, the ocean data assimilation has to compensate with a growing positive temperature increment (Figure 1).

In CERA-20C, the ocean and the atmosphere communicate every hour through the air–sea coupling at the outer-loop level of the variational method. Changes in the state of the atmosphere directly impact the ocean properties and vice versa. The combination of the coupled data assimilation and improvements in the atmospheric data assimilation corrects for the spurious trend in the net heat fluxes received by the ocean seen in ORA-20C. On average, heat flux and ocean temperature increments in CERA-20C oscillate around 0 W/m², suggesting a more balanced system.

CERA-20C production and output

B

The production of climate reanalyses requires large computing and archiving resources. To produce the CERA-20C dataset in a reasonable period of time, the period 1900–2010 was divided into 14 different streams of 10 years. Each production stream was initialised from the uncoupled reanalyses ERA-20C and ORA-20C. The first two years of each production stream were used for spin-up (only one-year of spin-up for the first stream) to produce the final climate dataset for the period 1901–2010.

The computation footprint of CERA-20C on ECMWF’s high-performance computing facility is significant, with seven months of production using 20,000 cores, which represents 5% of the total resources. 500,000 variational problems had to be solved processing up to 5,000,000 observations, at a pace of one every 30 seconds.

The evolution of the global weather for the period 1901–2010 is represented by a ten-member ensemble of 3-hourly estimates for ocean, surface and upper-air parameters. This represents more than 1,600 terabytes of data that had to be archived in ECMWF’s MARS archiving system.

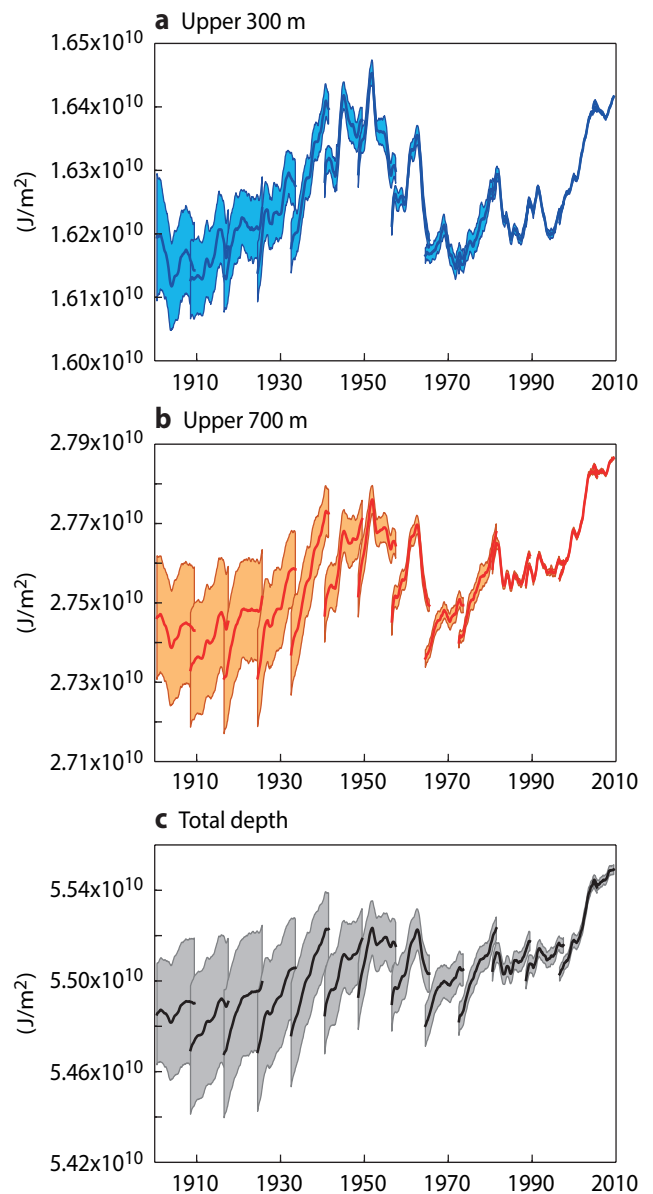


Figure 2 Time series of the global average ocean heat content in the CERA-20C ensemble for (a) the first 300 metres, (b) the first 700 metres and (c) the whole water column. The solid lines are the ensemble mean and the shading shows the ensemble spread.

Heat content

The evolution of ocean heat content over the 20th century is of particular interest as it has been identified in several studies as an indicator of ocean heat uptake, a process that is relevant to climate studies.

In CERA-20C, time series of heat content show discontinuities between streams resulting from the model drift from its initial state (Figure 2). The model drift reflects the fact that the initial conditions from ERA-20C and ORA-20C are inconsistent with the coupled model's natural state. In the early 20th century, when the uncertainty in the state of the ocean is high and the ocean model is poorly constrained by observations, the ocean component of CERA-20C drifts towards its preferred state. As the observing system grows, the uncertainty and the drift are reduced. The relatively well-observed upper ocean adjusts faster than the ocean interior, where the timescales of ocean processes are particularly slow and the observational constraints are very small. Further work is needed to understand and reduce the model drift so that the initial conditions and the ocean model behaviour are more realistic in poorly observed periods and areas.

Sea ice

Ocean–sea ice interactions through the LIM2 model have only recently been included in ECMWF's coupled model. ORA-20C provides a first record of sea-ice conditions for the 20th century in ocean-only mode while CERA-20C is the first application allowing these interactions in coupled mode on an interannual timescale.

Some issues in the settings of the sea-ice coupling to the atmosphere were found in CERA-20C. They translate into a lack of summer melting, leading to the accumulation of Arctic sea ice over the years. The sea-ice thickness in CERA-20C is over 5 metres in most of the Arctic basin, more than twice the expected average of 2 to 2.5 metres, as seen in ORA-20C (Figure 3a,b). A major impact on sea-ice extent is avoided thanks to the relaxation applied at the air–sea interface. A new configuration for the coupling between

sea ice and the atmosphere has been developed and tested. These coupled model experiments show a more realistic behaviour closer to the ocean-only mode (Figure 3c). Sea-ice interactions with the ocean and the atmosphere are highly sensitive processes and will need to be monitored carefully for future reanalysis.

Mean sea level pressure

New climate reanalyses need to be produced periodically to benefit from the latest updates in the models and data assimilation systems developed for numerical weather prediction. The scientific community and dataset users also provide feedback and raise important issues which need to be addressed in future reanalyses. This is why reanalysis is an ongoing activity that should never be regarded as completed.

Scientists have identified an issue in the general circulation in the southern hemisphere in ERA-20C and in the 20th-century atmospheric reanalysis produced by the US National Oceanic and Atmospheric Administration (20CR). The time series of mean sea level pressure (MSLP) decreases significantly between 1900 and 1950 over the Antarctic region, leading to a substantial strengthening of the polar vortex in the first half of the 20th century in these reanalyses (Figure 4). The development of CERA-20C, which is based on ERA-20C infrastructure, provided an opportunity to address this spurious climate drift.

In any data assimilation scheme, the specification of observation and background errors is crucial as it defines the weights used to blend together the information from the measurements and from the model. Specifying the observation error over the entire 20th century is not straightforward since measurement processes and representativeness errors are not well known. For this reason, it was decided to keep observation errors constant in ERA-20C (1.1 hPa for surface pressure and 1.5 hPa for mean sea level pressure). It has been found that those values are too small at the beginning of the century, giving too much weight to the observations. The assimilation adjusts the flow where it is the least constrained to improve the fit to observations. This produces large positive MSLP

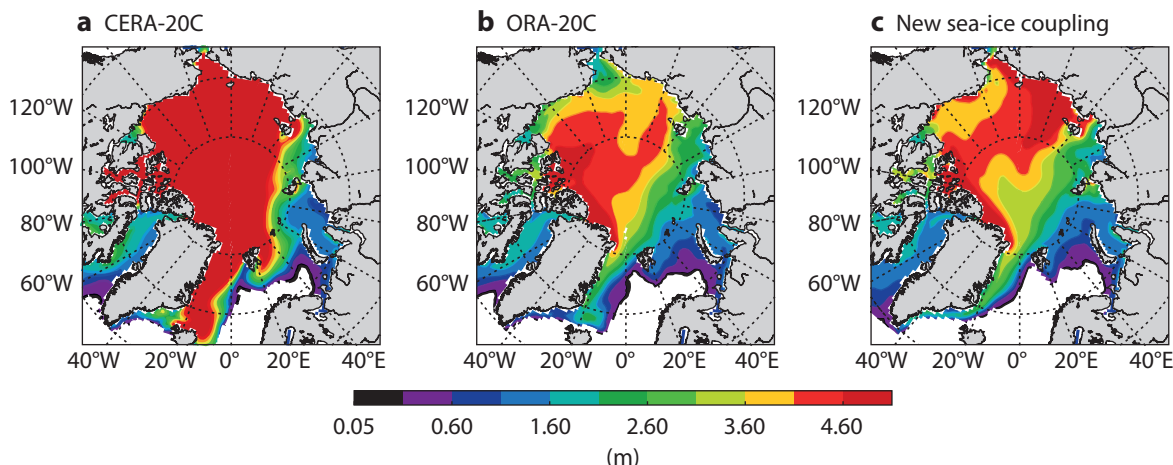


Figure 3 Arctic sea-ice thickness in March 1932 from (a) CERA-20C, (b) ORA-20C and (c) a coupled model run with new sea-ice coupling.

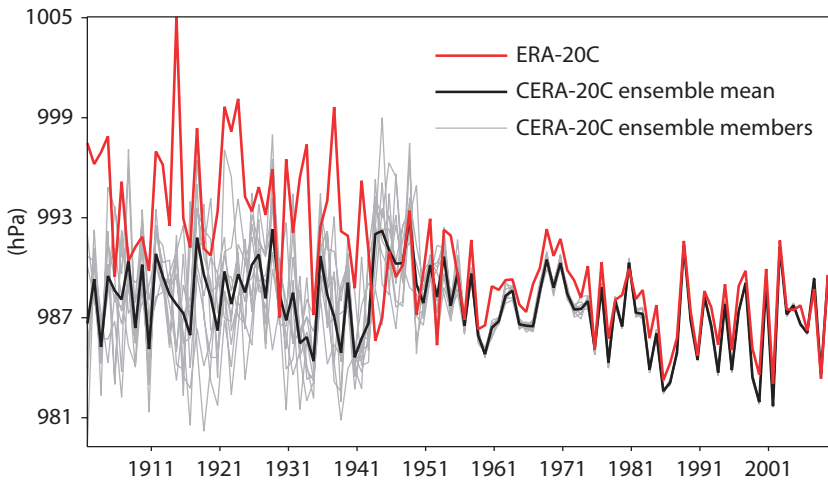


Figure 4 Time series of mean sea level pressure (MSLP) for the latitudes 90°S–60°S averaged over the period September–November each year.

increments over the Antarctic region resulting in too high MSLP values in the analysis (Figure 5). This behaviour disappears when the observing system becomes denser in the 1950s, with the first SYNOP stations in Antarctica and more observations from ships in the Antarctic Circle.

The Desroziers diagnostic (*Desroziers et al., 2005*) has been computed on the ERA-20C observation feedback statistics to estimate the a posteriori observation errors. The results show that a time-varying error would be more realistic.

The surface pressure error should vary from 1.6 hPa in 1900 to 0.8 hPa in 2010, while the MSLP error should vary from 2.0 hPa in 1900 to 1.2 hPa in 2010.

For the production of CERA-20C, observation errors were adjusted in accordance with the results of the Desroziers

diagnostic. A larger observation error at the beginning of the century causes the assimilation to fit the model data slightly less closely to the observations and prevents large increments over the Antarctic region. As a result, the CERA-20C ensemble mean looks more realistic with better consistency in the climate trends. The larger ensemble spread at the beginning of the century reflects the larger uncertainties in the climate reconstruction as the region is poorly observed before the 1950s.

Ensemble technique

For the first time, CERA-20C provides a ten-member ensemble climate reanalysis for all parameters and levels over the 20th century. Ensemble generation is based on the Ensemble of Data Assimilations (EDA) system developed

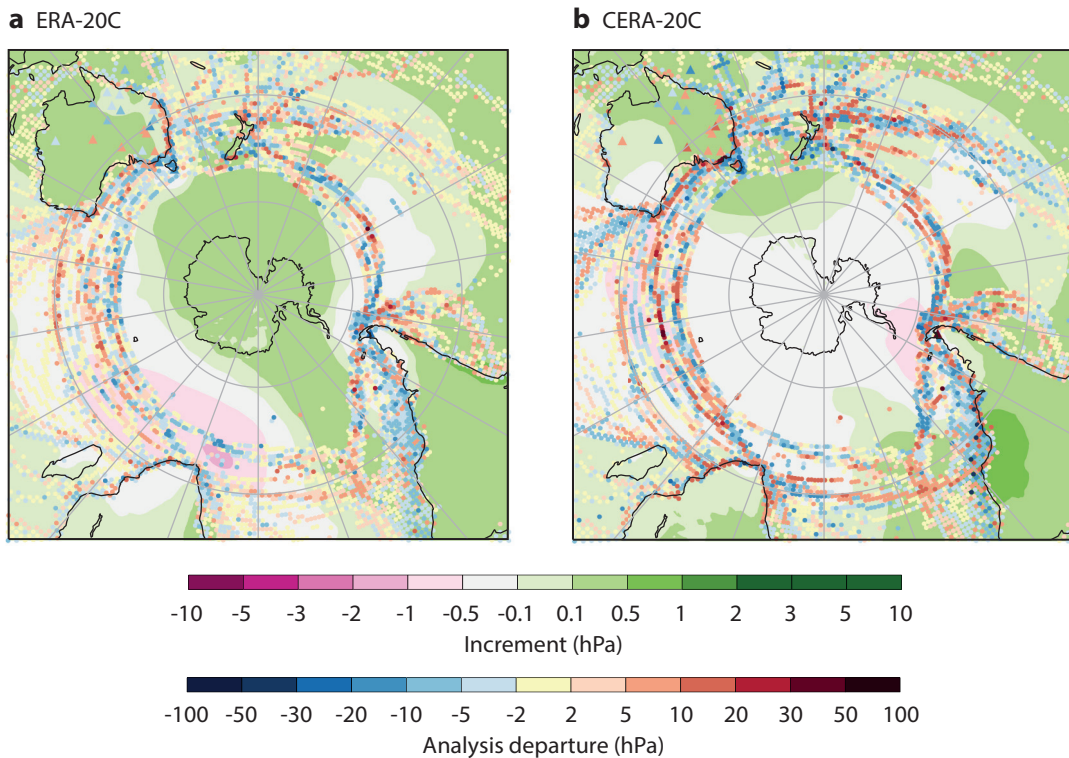


Figure 5 Mean sea level pressure increments (shading) for the year 1924 in (a) ERA-20C and (b) CERA-20C. Dots and triangles represent the difference between the analysis and mean sea level pressure observations and surface pressure observations, respectively (analysis departures).

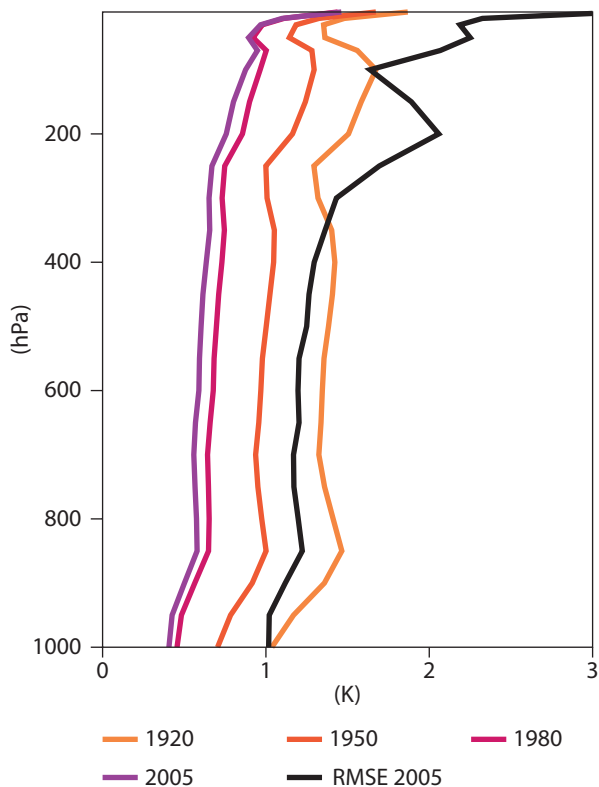


Figure 6 Vertical profiles of the standard deviation of the CERA-20C ensemble for temperature over 60°S–60°N for the years 1920, 1950, 1980 and 2005. The root-mean-square error (RMSE) of the CERA-20C ensemble mean compared to ERA-Interim in 2005 has been plotted for comparison.

at ECMWF and Météo-France, which explicitly accounts for errors in the observational record and in the forecast model. The information from the ten members is used during the assimilation to compute a flow-dependent background error, which determines how to spread the information from observations in space.

The ensemble technique also aims to provide an indication of the confidence we can have in the data. The ensemble standard deviation is equal to 1.0°C at 1,000 hPa in 1920 and reduces to 0.4°C in 2005 (Figure 6). The ensemble spread in CERA-20C gradually decreases over time, which indicates that we can have more confidence in the data

as more observations become available. The greater observation density means that synoptic weather charts in CERA-20C are much better near the end of the century than at the beginning.

The analysis ensemble spread is supposed to represent the error of the analysis ensemble mean and should ideally be equal to the root-mean-square error (RMSE) of the ensemble mean compared to the true atmospheric state. This has been verified for the year 2005, when ERA-Interim provides a good proxy for the truth as it assimilates all types of observation at a higher resolution. Maps of the ensemble spread and of the RMSE show very similar horizontal structures, which means that the EDA correctly captures where the uncertainties are. However, the RMSE of CERA-20C is about twice as large as the CERA-20C analysis ensemble spread. This global offset between the spread and RMSE can be seen in the vertical profiles (Figure 6). CERA-20C is thus overly confident in the data compared to the actual error. It is important to note that this diagnostic has some limitations as it is based on a proxy of the truth. To improve the uncertainty estimations in CERA-20C, the size of the ensemble and the way the perturbations are generated in the different members when the EDA system is used for climate reanalysis will require further investigation.

Access to the data and outlook

The multiple production streams have been consolidated excluding the spin-up years to produce the final released climate dataset. An automatic procedure has checked the data for continuity over time and has verified that not a single field is missing. The data server (<http://apps.ecmwf.int/datasets>) provides an interface similar to that of ERA-Interim. Users can select parameters and time periods of interest for download. For large retrievals, scripts are available to download data in batch mode. Users will be able to access the ensemble mean and spread to characterise uncertainties in their own applications.

As indicated in this article, ECMWF has already begun to analyse the data and to identify ways in which future 20th-century global reanalyses can be improved. When users elsewhere obtain the data and provide feedback or publish their findings, they will help improve the way future reanalyses are produced, thereby benefiting climate research and societal applications.

FURTHER READING

- de Boissésou, E. & M. Balmaseda**, 2016: An ensemble of 20th century ocean reanalyses for providing ocean initial conditions for CERA-20C coupled streams. *ERA report series*, **24**.
- Desroziers, G., L. Berre, B. Chapnik, P. Poli**, 2005: Diagnosis of observation, background and analysis-error statistics in observation space. *Q.J.R. Meteorol. Soc.*, **133**, 3385–3396, doi:10.1256/qj.05.108.
- Hersbach, H., D. Dee**, 2016: ERA5 reanalysis is in production. *ECMWF Newsletter No. 147*, 7.

- Laloyaux, P., D. Dee**, 2015: CERA: A coupled data assimilation system for climate reanalysis. *ECMWF Newsletter No. 144*, 15–20.
- Laloyaux, P., M. Balmaseda, D. Dee, K. Mogensen & P. Janssen**, 2016: A coupled data assimilation system for climate reanalysis. *Q. J. R. Meteorol. Soc.*, **142**, 65–78.
- Poli, P., H. Hersbach, D. Dee, P. Berrisford, A. Simmons, F. Vitart, P. Laloyaux, D. Tan, C. Peubey, J.-N. Thépaut, Y. Trémolet, E. Holm, M. Bonavita, L. Isaksen & M. Fisher**, 2016: ERA-20C: An Atmospheric Reanalysis of the Twentieth Century. *Journal of Climate*, **29**, 4083–4097.

doi:10.21957/t4znuhb842

Twenty-one years of wave forecast verification

JEAN-RAYMOND BIDLOT

Routine comparisons of wave forecast data from different models were first informally established in 1995. They were intended to provide a mechanism for assessing the quality of operational wave forecast model output. The comparisons were based on an exchange of model analysis and forecast data at the locations of in-situ observations of significant wave height, wave period and wind speed and direction available via the Global Telecommunication System (GTS). Five European and North American institutions routinely running wave forecast models contributed to that exchange (*Bidlot et al.*, 1998). The Expert Team on Wind Waves and Storm Surges of the Joint Technical Commission for Oceanography and Marine Meteorology (JCOMM) noted the value of the exchange during its first meeting in Halifax, Canada, in June 2003 and endorsed the expansion of the scheme to include other wave forecasting systems. The exchange was subsequently expanded to other global wave forecasting centres and a few regional entities (Table 1).

A review of 21 years of wave verification results shows clear improvements in the quality of wave forecasting, as will be illustrated in this article for significant wave height forecasts. The comparison project has benefitted all participants and should continue to do so. However, the informal character of the exchange prevents a rapid adaptation to new data. For these reasons, the World Meteorological Organization (WMO) is seeking to establish a Lead Centre for Wave Forecast Verification (LC-WFV) with clearly defined interfaces between the participants and the Lead Centre. ECMWF has expressed its interest in becoming the designated Lead Centre.

Data

On a monthly basis, each participating centre provides time series of model data at an agreed list of locations to ECMWF, where the data are collated for subsequent access. Observations are also collected at ECMWF. The combined data are then processed to provide summary statistics. These are made available on the ECMWF website (<http://www.ecmwf.int/en/forecasts/charts/>) and the JCOMM website (<http://www.jcomm.info/>). The raw data are also made available to all participants for potential further analysis.

Sea state and ocean surface meteorological in-situ observations are routinely collected by several national organisations via networks of moored buoys or weather ships and fixed platforms deployed in their near-shore and offshore areas of interest. The data are usually exchanged via the GTS. As part of this intercomparison, observations that are not commonly available on the GTS are also gathered on a case-by-case basis. The geographical coverage of the wave data is still very limited. It tends to be limited to areas near the coast and some observations

are very close to land. At the present global wave model resolution, only a subset of these locations fall within the wave model grids. Most measurements used in this project are made in the northern hemisphere (see Figure 4 for recent coverage).

Before using observations for verification, care has to be taken to process the data to remove any erroneous observations. It is also necessary to match the temporal scale of model data and observations. This scale matching is achieved by averaging the hourly observation data in time windows centred on verifying times. The original quality control and averaging procedure was discussed in *Bidlot et al.* (2002). It was extended to include platform data as described in *Sætra & Bidlot* (2004).

The intercomparison relies on the exchange of model output at a list of locations. Because in-situ networks change over time, updates to the list have been necessary. However, not all participants have been able to update their list at the same time, nor do they provide data for all the same locations. Moreover, some participants only run a limited-area model, use a coarser grid or provide data from a different number of forecasts (Table 1). A fair comparison between the different wave forecasting systems can only be achieved if the same observation–model collocations are used. This constrains the number of systems that can be evaluated at any one time.

Over 20 years of progress

Figure 1a shows the significant wave height forecast skill from September 2015 to August 2016 as measured by the scatter index (Box A) for all systems providing global forecasts from 00 UTC (see Table 1). Figure 1b shows the common locations and the data coverage density (the number of observation–model collocations used relative to

Scatter index

A

The scatter index is a measure of the size of the deviation of forecasts from observations relative to the magnitude of the observations. It is normally given in per cent. A smaller scatter index value means better forecasts.

Mathematically the scatter index is defined as the standard deviation of the difference between predicted values and observations normalised by the mean of the observations. For example, if the standard deviation of the difference between predicted values of significant wave height and observations is 0.5 metres and the mean of the observations is 2 metres, then the scatter index value is $0.5/2$, which is 25%.

Significant wave height is defined as four times the square root of the integral of the wave spectrum. It closely corresponds to the average height of the highest one third of waves.

	Organisation	Acronym	Start date	Coverage	Forecasts per day	Forecast range (days)
1	European Centre for Medium-Range Weather Forecasts, UK	ECMWF	Jun 1995	global	2	10
2	Met Office, UK	UKMO	Jun 1995	global	2	5
3	Fleet Numerical Meteorology and Oceanography Center, USA	FNMOOC	Jun 1995	global	4	6
4	Environment and Climate Change Canada, Canada	ECCC	Jun 1995	regional until June 2015, then global	2	5
5	National Centers for Environmental Prediction, USA	NCEP	May 1996	global	4	7
6	Météo France, France	METFR	Jan 2001	global	2	5
7	Deutscher Wetterdienst, Germany	DWD	Feb 2004	global	2	5
8	Bureau of Meteorology, Australia	BoM	Sep 2005	global	2	5
9	Service Hydrographique et Océanographique de la Marine, France	SHOM	Sep 2006	global	2	6
10	Japan Meteorological Agency, Japan	JMA	Sep 2006	global	4/1	3.5/10
11	Korea Meteorological Administration, Republic of Korea	KMA	Jan 2007	global	2	10
12	Puertos del Estado, Spain	PRTOS	Jan 2007	regional	2	3
13	Danmarks Meteorologiske Institut, Denmark	DMI	Jan 2010	regional	4	5
14	National Institute of Water and Atmospheric Research, New Zealand	NIWA	Jun 2010	global	1	6
15	Det Norske Meteorologiske Institutt, Norway	METNO	Feb 2011	regional	4	2
16	Servicio de Hidrografía Naval, Servicio Meteorológico, Argentina	SHNSM	Aug 2011	regional	2	4

Table 1 Current contributors to the wave forecast verification project. The start date indicates the date from which data have been provided. Data coverage is either global or regional. The number of forecasts per day and the forecast range refer to the data that is transmitted for verification purposes and not to what each centre provides to its users.

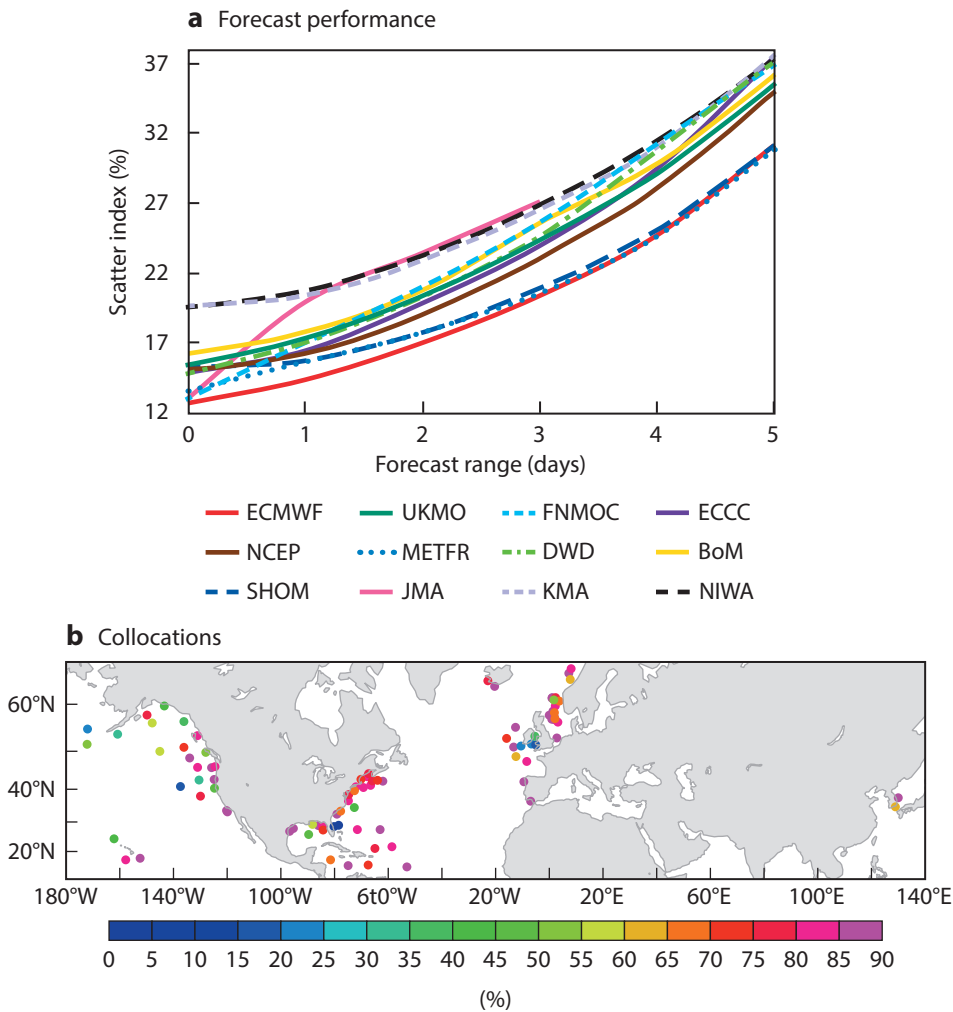


Figure 1 Forecast performance of different centres for forecasts initialised at 00 UTC and 12 UTC between September 2015 and August 2016, showing (a) the scatter index (%) for significant wave height when compared to buoy observations for different forecast ranges and (b) the buoy positions and the number of observation-model collocations used relative to the maximum number of possible collocations over this one-year period.

the maximum number of possible collocations). This article does not aim to explain why each forecasting system performs differently. Rather, it aims to illustrate the remarkable progress that has been made over the years (Figures 2 and 3). Progress might have come from improvements in atmospheric forcing resulting from a collective effort in developing numerical weather prediction (NWP) systems, and/or advances in the wave model physical parametrizations, numerical methods, data assimilation or improved implementation. It is, however, worth mentioning that METFR and SHOM both use winds from ECMWF, which explains their close similarity with ECMWF in terms of forecast performance.

Figure 2a shows the evolution of 5-year running mean scatter index values for day-5 significant wave height forecasts for an area of the North-East Pacific. The selected offshore buoys have been part of the intercomparison since the early years. The plot was produced with consistent 00 and 12 UTC forecasts at all selected locations. The data

coverage density over the full period is also shown (Figure 2b). It is not entirely uniform but the locations have been carefully selected to reflect the wave climate of the area. The decrease in scatter index values is a clear indication of the steady improvements made by all participating centres. There is a degree of convergence in model performance since 2009. Comparable results also hold for shorter forecast ranges (not shown). Similarly, other ocean areas with long-term observational coverage, such as the North-West Atlantic, the North-East Atlantic and the North Sea, generally show the same improving trend for all participants and forecast ranges (Figure 3a–c). However, for enclosed areas such as the Western Mediterranean Sea, progress has been less consistent (Figure 3d).

ECMWF data can be collocated with all available in-situ data. Figure 4 shows that enclosed areas and near-shore locations are indeed much more difficult to model, in particular on the western side of all ocean basins. This is not limited to ECMWF but is a feature of forecasts from

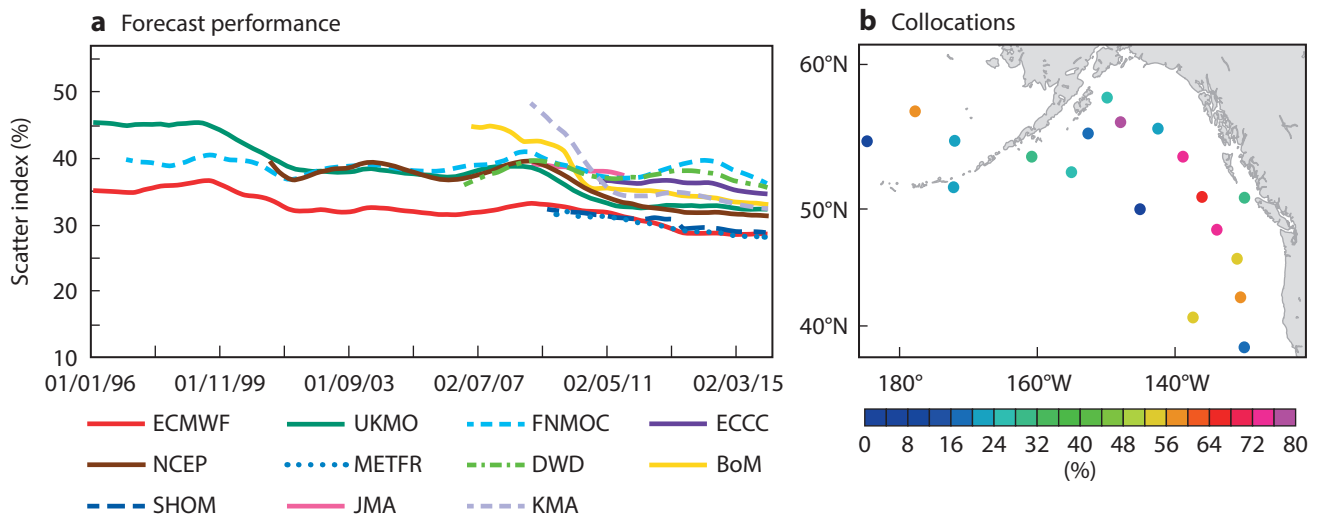


Figure 2 Forecast performance of different centres for forecasts initialised at 00 UTC and 12 UTC showing (a) the long-term evolution of 5-year running mean scatter index values for day-5 significant wave height forecasts when compared to buoy observations over the North-East Pacific and (b) the buoy positions and the number of observation–model collocations used relative to the maximum number of possible collocations over the 21-year period.

all centres (Figure 5). Nonetheless, the quality of wave forecasting as a whole has improved quite dramatically. There is obviously room for further advances. It is believed that institutions engaged in wave forecasting will continue to benefit from this type of inter-validation in the same way as NWP centres have benefitted from the exchange of forecast verification scores under the auspices of the WMO.

Outlook

There has been a slow, yet steady increase in the availability of in-situ wave observations. Space-borne altimeter wave height data have been shown to be of very high quality and are now commonly available (Abdalla & Zuo, 2016). The intercomparison should ideally be extended to include these data. The JCOMM Expert Team on Waves and Coastal Hazards has recommended that the current Wave Forecast Verification project should be formalised by establishing a Lead Centre for Wave Forecast Verification (LC-WFV). ECMWF has responded positively to this request. The designated LC-WFV would coordinate efforts to gather a set of selected model fields relevant to wave forecasting activities under an agreed data exchange protocol. Once the process of gathering the relevant fields is in place, the routine verification against in-situ data will be more flexible and adaptive. Moreover, it will become much easier to include new observational datasets and verification metrics.

The author would like to thank Andy Saulter (UK Met Office), Paul Wittmann (FNMOC), Natacha Bernier (ECCC), Arun Chawla (NCEP), Lotfi Aouf (Météo-France), Thomas Bruns (DWD), Aihong Zhong (BoM), Fabrice Arduin (SHOM), Nadao Kohno (JMA), Sanwook Park (KMA), José María García-Valdecasas Bernal (PRTOS), Jacob Woge Nielsen (DMI), Richard Gorman (NIWA), Ana Carrasco (METNO) and Paula Etala (SHNSM) for their contribution to the comparison project and for providing the data that has made this article possible.

FURTHER READING

Abdalla, S. & H. Zuo, 2016: The use of radar altimeter products at ECMWF. *ECMWF Newsletter No. 149*, 14–19.

Bidlot, J.-R., M. Holt, P.A. Wittmann, R. Lalbeharry & H.S. Chen, 1998: Towards a systematic verification of operational wave models. *Proceedings Third Int. Symposium on WAVES97: November 3-7, 1997*, Virginia Beach: American Society of Civil Engineers.

Bidlot, J.-R., D.J. Holmes, P.A. Wittmann, R. Lalbeharry & H.S. Chen, 2002: Intercomparison of the performance of operational ocean wave forecasting systems with buoy data. *Wea. Forecasting*, **17**, 287–310.

Sætra, Ø. & J.-R. Bidlot, 2004: On the potential benefits of using probabilistic forecasts for waves and marine winds based on the ECMWF ensemble prediction system. *Wea. Forecasting*, **19**, 673–689.

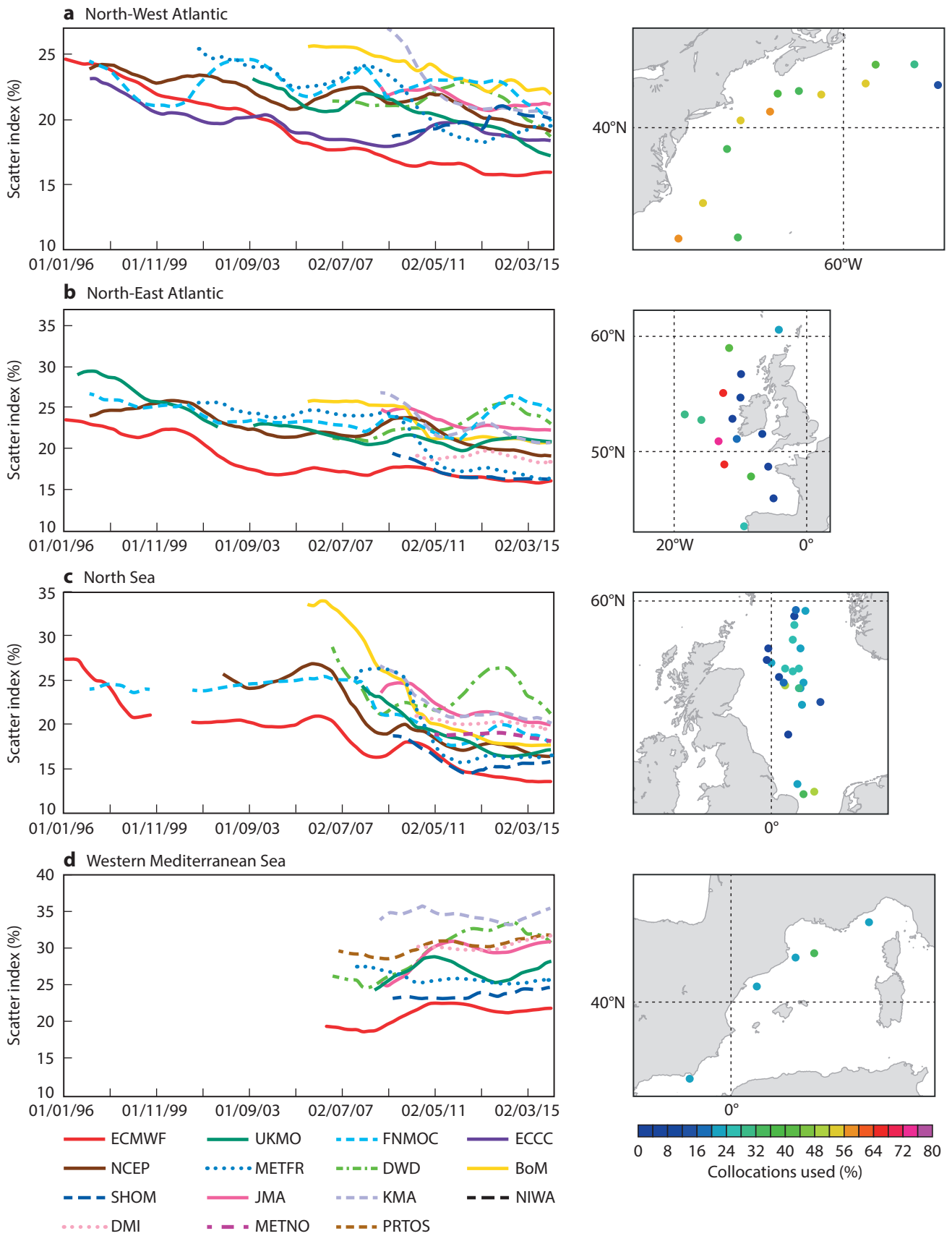


Figure 3 Same as Figure 2 but for (a) day-1 forecasts for the North-West Atlantic, (b) day-3 forecasts for the North-East Atlantic, (c) day-1 forecasts for the North Sea, and (d) day-1 forecasts for the Western Mediterranean Sea, for different sets of forecasting centres.

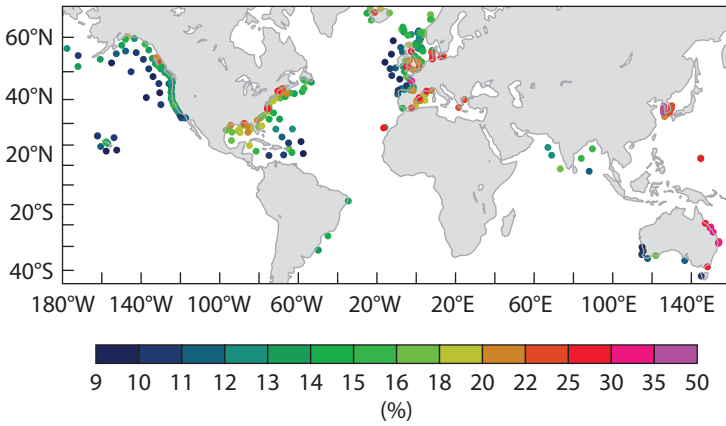


Figure 4 Scatter index for day-1 ECMWF forecasts of significant wave height initialised at 00 and 12 UTC every day from September 2015 to August 2016 compared to buoy observations, shown for each buoy location.

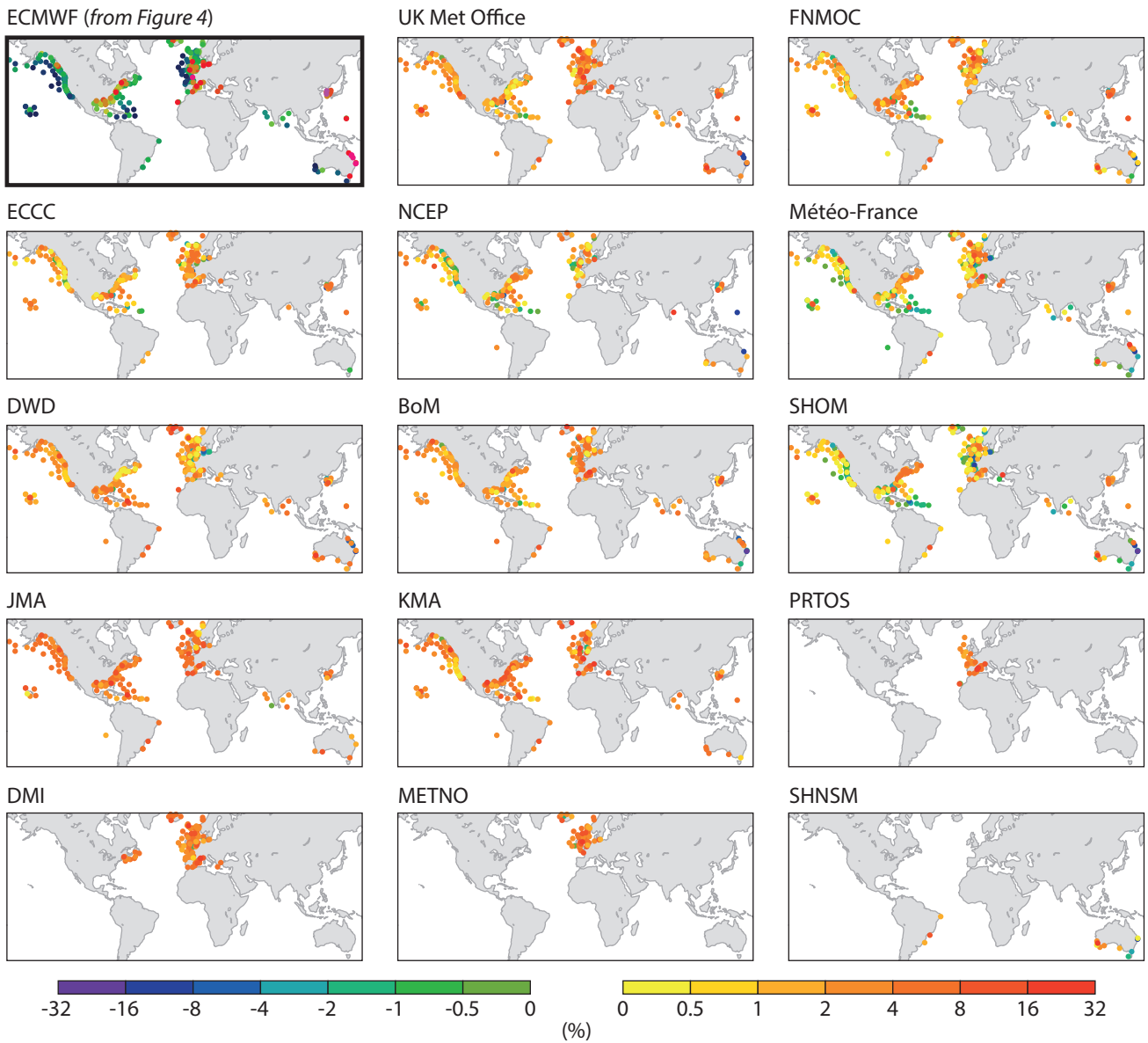


Figure 5 The top left panel shows scatter index values for ECMWF day-1 significant wave height forecasts as in Figure 4. The other panels show the difference in scatter index expressed in per cent with respect to ECMWF at each location from other participating centres to the extent that data were available from September 2015 to August 2016.

ECMWF Council and its committees

The following provides some information about the responsibilities of the ECMWF Council and its committees. More details can be found at:

<http://www.ecmwf.int/en/about/who-we-are/governance>

Council

The Council adopts measures to implement the ECMWF Convention; the responsibilities include admission of new members, authorising the Director-General to negotiate and conclude co-operation agreements, and adopting the annual budget, the scale of financial contributions of the Member States, the Financial Regulations and the Staff Regulations, the long-term strategy and the programme of activities of the Centre.



President Prof. Miguel Miranda (Portugal)

Vice President Prof. Juhani Damski (Finland)

Policy Advisory Committee (PAC)

The PAC provides the Council with opinions and recommendations on any matters concerning ECMWF policy submitted to it by the Council, especially those arising out of the four-year programme of activities and the long-term strategy.



Chair Mrs Marianne Thyrring (Denmark)

Vice Chair Mr Rolf Brennerfelt (Sweden)

Finance Committee (FC)

The FC provides the Council with opinions and recommendations on all administrative and financial matters submitted to the Council and exercises the financial powers delegated to it by the Council.



Chair Mr Marko Viljanen (Finland)

Vice Chair Mr Mark Hodkinson (United Kingdom)

Scientific Advisory Committee (SAC)

The SAC provides the Council with opinions and recommendations on the draft programme of activities of the Centre drawn up by the Director-General and on any other matters submitted to it by the Council. The 12 members of the SAC are appointed in their personal capacity and are selected from among the scientists of the Member States.



Chair Prof. Alan O'Neill (United Kingdom)

Vice Chair Prof. Wilco Hazeleger (The Netherlands)

Technical Advisory Committee (TAC)

The TAC provides the Council with advice on the technical and operational aspects of the Centre including the communications network, computer system, operational activities directly affecting Member States, and technical aspects of the four-year programme of activities.



Chair Mr Jean-Marie Carrière (France)

Vice Chair Dr Philippe Steiner (Switzerland)

Advisory Committee for Data Policy (ACDP)

The ACDP provides the Council with opinions and recommendations on matters concerning ECMWF Data Policy and its implementation.



Chair Mr Søren Olufsen (Denmark)

Vice Chair Mr Francisco Pascual Perez (Spain)

Advisory Committee of Co-operating States (ACCS)

The ACCS provides the Council with opinions and recommendations on the programme of activities of the Centre, and on any matter submitted to it by the Council.



Chair Dr Václav Dvořák (Czech Republic)

Vice Chair Mr Taimar Ala (Estonia)

ECMWF Calendar 2017

Jan 23–27	Computer User Training Course: HPC Facility Cray XC40
Jan 30–3 Feb	Training Course for Trainers, Training Champions: Use and Interpretation of ECMWF Products
Feb 6–10	Training Course: Use and Interpretation of ECMWF Products
Feb 20–24	Computer User Training Course: Introduction for New Users/ MARS
Feb 28	Council, Extraordinary Session
Feb 28–1 Mar	Workshop on Data Policy
Feb 28–3 Mar	Computer User Training Course: ecCodes, GRIB
Mar 1–3	Workshop on Meteorological Operational Systems
Mar 4–5	Hackathon on Open Data
Mar 6–9	Computer User Training Course: ecCodes, BUFR
Mar 13–17	NWP Training Course: Advanced Numerical Methods for Earth System Modelling
Mar 20–24	NWP Training Course: Parametrization of Subgrid Physical Processes
Mar 27–31	NWP Training Course: Data Assimilation
Apr 3–7	EUMETSAT/ECMWF NWP SAF Training Course: Assimilation of Satellite Data

Apr 4	EUMETSAT Data Policy Group
Apr 5	Advisory Committee for Data Policy
Apr 5–6	ECOMET Working Group
Apr 24	Policy Advisory Committee
Apr 25–26	Finance Committee
May 8–12	NWP Training Course: Predictability and Ocean–Atmosphere Ensemble Forecasting
May 16–17	Security Representatives' Meeting
May 17–19	Computing Representatives' Meeting
Jun 12–16	Using ECMWF's Forecasts (UEF)
Jun 21–22	Council
Sep 11–14	Annual Seminar
Oct 2–5	Training Course: Use and Interpretation of ECMWF Products
Oct 9–11	Scientific Advisory Committee
Oct 12–13	Technical Advisory Committee
Oct 16	Policy Advisory Committee
Oct 17–18	Finance Committee
Oct 25	Advisory Committee of Co-operating States
Dec 7–8	Council

Contact information

ECMWF, Shinfield Park, Reading, Berkshire RG2 9AX, UK

Telephone National 0118 949 9000

Telephone International +44 118 949 9000

Fax +44 118 986 9450

ECMWF's public website <http://www.ecmwf.int/>

E-mail: The e-mail address of an individual at the Centre is firstinitial.lastname@ecmwf.int. For double-barrelled names use a hyphen (e.g. j-n.name-name@ecmwf.int).

Problems, queries and advice	Contact
General problems, fault reporting, web access and service queries	servicedesk@ecmwf.int
Advice on the usage of computing and archiving services	advisory@ecmwf.int
Queries regarding access to data	data.services@ecmwf.int
Queries regarding the installation of ECMWF software packages	software.support@ecmwf.int
Queries or feedback regarding the forecast products	forecast_user@ecmwf.int

ECMWF publications

(see <http://www.ecmwf.int/en/research/publications>)

Technical Memoranda

- 792 **Haiden, T., M. Janousek, J. Bidlot, L. Ferranti, F. Prates, F. Vitart, P. Bauer, D.S. Richardson:** Evaluation of ECMWF forecasts, including the 2016 resolution upgrade. *December 2016*
- 791 **Mueller, A., E. Dutra, H. Cloke, A. Verhoef, G. Balsamo, F. Pappenberger:** Water infiltration and redistribution in Land Surface Models. *November 2016*
- 790 **Di Giuseppe, F., S. Remy, F. Pappenberger, F. Wetterhall:** Improving GFAS and CAMS biomass burning estimations by means of the Global ECMWF Fire Forecast system (GEFF). *December 2016*
- 789 **Chen, K., N. Bormann, S. English, J. Zhu:** Assimilation of MWHS data over Land. *November 2016*
- 788 **Ruggieri, P., R. Buizza, G. Visconti:** On the link between Barents-Kara sea-ice variability and European blocking. *November 2016*
- 787 **Hogan, R.J., A. Bozzo:** ECRAD: A new radiation scheme for the IFS. *November 2016*
- 786 **Janiskova, M., C. Cardinali:** On the impact of the diabatic component in the Forecast Sensitivity Observation Impact diagnostics. *August 2016*
- 785 **Leutbecher, M., S.J. Lock, P. Ollinaho, S.T.K. Lang, G.P. Balsamo, P. Bechtold:** Stochastic representations of model uncertainties at ECMWF: State of the art and future vision. *December 2016*

ERA Report Series

- 26 **Hirahara, S., M. Alonso Balmaseda, E. de Boisseson, H. Hersbach:** Sea Surface Temperature and Sea Ice Concentration for ERA5. *2016*

ESA Contract Report

- Janiskova, M., M. Fielding:** Operational Assimilation of Space-borne Radar and Lidar Cloud Profile Observations for Numerical Weather Prediction: WP-1000 report: Preliminary analysis and Planning. *2016*

Index of Newsletter articles

This is a selection of articles published in the *ECMWF Newsletter* series during recent years.

Articles are arranged in date order within each subject category.

Articles can be accessed on ECMWF's public website – <http://www.ecmwf.int/en/research/publications>

	No.	Date	Page		No.	Date	Page
NEWS							
Flash floods over Greece in early September 2016	150	Winter 2016/17	2	Copernicus Climate Change Service tracks record global temperatures	149	Autumn 2016	7
ECMWF widens role in WMO severe weather projects	150	Winter 2016/17	4	Experts discuss role of drag processes in NWP and climate models	149	Autumn 2016	8
New opportunities from HEO satellites	150	Winter 2016/17	5	ECMWF hosts Year of Polar Prediction meeting	149	Autumn 2016	9
Lakes in weather prediction: a moving target	150	Winter 2016/17	6	ECMWF releases software for observational data	149	Autumn 2016	10
New Director of Research appointed	150	Winter 2016/17	7	Survey shows MARS users broadly satisfied	149	Autumn 2016	11
New Council President elected	150	Winter 2016/17	7	Supercomputing project reviews performance analysis tools	149	Autumn 2016	12
ERA5 aids in forecast performance monitoring	150	Winter 2016/17	8	ANYWHERE and IMPREX hold general assemblies	149	Autumn 2016	13
ECMWF to work with RIMES on flood forecasting	150	Winter 2016/17	8	New Strategy is "ambitious but not unrealistic"	148	Summer 2016	2
Scientists discuss methods to simulate all-scale geophysical flows	150	Winter 2016/17	9	Forecasts showed Paris flood risk well in advance	148	Summer 2016	4
C3S trials seasonal forecast service	150	Winter 2016/17	10	Better temperature forecasts along the Norwegian coast	148	Summer 2016	6
Multi-decadal variability in predictive skill of the winter NAO	150	Winter 2016/17	11	Atmospheric composition forecasts move to higher resolution	148	Summer 2016	7
ECMWF meets Ibero-American weather services	150	Winter 2016/17	12	OBE for Alan Thorpe	148	Summer 2016	7
Experts debate future of supercomputing in meteorology	150	Winter 2016/17	13	New satellite data reduce forecast errors	148	Summer 2016	8
Météo-France hosts OpenIFS workshop	149	Autumn 2016	2	ECMWF steps up assimilation of aircraft weather data	148	Summer 2016	10
Predicting heavy rainfall in China	149	Autumn 2016	4	GloFAS meeting supports integrated flood forecasting	148	Summer 2016	11
ECMWF makes S2S forecast charts available	149	Autumn 2016	5				
Graduate trainees enjoyed their time at ECMWF	149	Autumn 2016	6				

	No.	Date	Page
First Scalability Day charts way forward	148	Summer 2016	13
Evaluating forecasts tops agenda at 2016 user meeting	148	Summer 2016	14
First Women in Science Lunch held at ECMWF	148	Summer 2016	15
New Director of Forecasts appointed	148	Summer 2016	16
Croatian flag raised at ECMWF	148	Summer 2016	16
Web standards for easy access to big data	148	Summer 2016	17
Joint work with CMA leads to second S2S database	148	Summer 2016	18
ECMWF takes part in WMO data monitoring project	148	Summer 2016	19
Wind and wave forecasts during Storm Gertrude/Tor	147	Spring 2016	2
Forecasts aid mission planning for hurricane research	147	Spring 2016	3
ECMWF helps to probe impact of aerosols in West Africa	147	Spring 2016	5
Croatian flag to be raised at the Centre on 30 June	147	Spring 2016	6
ERA5 reanalysis is in production	147	Spring 2016	7
Supercomputer upgrade is under way	147	Spring 2016	8
ECMWF steps up work on I/O issues in supercomputing	147	Spring 2016	8
The Copernicus Climate Change Service Sectoral Information Systems	147	Spring 2016	9
Hackathon aims to improve Global Flood Awareness System	147	Spring 2016	11
'Training the trainer' in the use of forecast products	147	Spring 2016	12
Alan Thorpe's legacy at ECMWF	146	Winter 2015/16	2
Forecasting flash floods in Italy	146	Winter 2015/16	3
Forecast performance 2015	146	Winter 2015/16	5
Tropical cyclone forecast performance	146	Winter 2015/16	7
Monitoring the 2015 Indonesian fires	146	Winter 2015/16	8
Visualising data using ecCharts: a user perspective	146	Winter 2015/16	9
Forecasts aid flood action in Peru during El Niño	146	Winter 2015/16	10
Calibrating river discharge forecasts	146	Winter 2015/16	12
CERA-20C production has started	146	Winter 2015/16	13
Migration to new ECMWF website is complete	146	Winter 2015/16	15
Software updates in preparation for model cycle 41r2	146	Winter 2015/16	16
Forty years of improving global forecast skill	145	Autumn 2015	2
Predicting this year's European heat wave	145	Autumn 2015	4
ECMWF meets its users to discuss forecast uncertainty	145	Autumn 2015	6
Trans-polar transport of Alaskan wildfire smoke in July 2015	145	Autumn 2015	8
VIEWPOINT			
Living with the butterfly effect: a seamless view of predictability	145	Autumn 2015	18
Decisions, decisions...!	141	Autumn 2014	12
Using ECMWF's Forecasts: a forum to discuss the use of ECMWF data and products	136	Summer 2013	12
Describing ECMWF's forecasts and forecasting system	133	Autumn 2012	11

	No.	Date	Page
COMPUTING			
ECMWF's new data decoding software ecCodes	146	Winter 2015/16	35
Supercomputing at ECMWF	143	Spring 2015	32
SAPP: a new scalable acquisition and pre-processing system at ECMWF	140	Summer 2014	37
Metview's new user interface	140	Summer 2014	42
GPU based interactive 3D visualization of ECMWF ensemble forecasts	138	Winter 2013/14	34
RMDCN – Next Generation	134	Winter 2012/13	38
METEOROLOGY			
OBSERVATIONS & ASSIMILATION			
CERA-20C: An Earth system approach to climate reanalysis	150	Winter 2016/17	25
The use of radar altimeter products at ECMWF	149	Autumn 2016	14
Joint project trials new way to exploit satellite retrievals	149	Autumn 2016	20
Global radiosonde network under pressure	149	Autumn 2016	25
Use of forecast departures in verification against observations	149	Autumn 2016	30
Use of high-density observations in precipitation verification	147	Spring 2016	20
GEOVOW project boosts access to Earth observation data	145	Autumn 2015	35
CERA: A coupled data assimilation system for climate reanalysis	144	Summer 2015	15
Promising results in hybrid data assimilation tests	144	Summer 2015	33
Snow data assimilation at ECMWF	143	Spring 2015	26
Assimilation of cloud radar and lidar observations towards EarthCARE	142	Winter 2014/15	17
The direct assimilation of principal components of IASI spectra	142	Winter 2014/15	23
Automatic checking of observations at ECMWF	140	Summer 2014	21
All-sky assimilation of microwave humidity sounders	140	Summer 2014	25
Climate reanalysis	139	Spring 2014	15
Ten years of ENVISAT data at ECMWF	138	Winter 2013/14	13
Impact of the Metop satellites in the ECMWF system	137	Autumn 2013	9
Ocean Reanalyses Intercomparison Project (ORA-IP)	137	Autumn 2013	11
The expected NWP impact of Aeolus wind observations	137	Autumn 2013	23
Winds of change in the use of Atmospheric Motion Vectors in the ECMWF system	136	Summer 2013	23
FORECAST MODEL			
New IFS cycle brings sea-ice coupling and higher ocean resolution	150	Winter 2016/17	14
Impact of orographic drag on forecast skill	150	Winter 2016/17	18
Single-precision IFS	148	Summer 2016	20
New model cycle brings higher resolution	147	Spring 2016	14
Reducing systematic errors in cold-air outbreaks	146	Winter 2015/16	17
A new grid for the IFS	146	Winter 2015/16	23
An all-scale, finite-volume module for the IFS	145	Autumn 2015	24

	No.	Date	Page
Reducing surface temperature errors at coastlines	145	Autumn 2015	30
Atmospheric composition in ECMWF's Integrated Forecasting System	143	Spring 2015	20
Towards predicting high-impact freezing rain events	141	Autumn 2014	15
Improving ECMWF forecasts of sudden stratospheric warmings	141	Autumn 2014	30
Improving the representation of stable boundary layers	138	Winter 2013/14	24
Interactive lakes in the Integrated Forecasting System	137	Autumn 2013	30
Effective spectral resolution of ECMWF atmospheric forecast models	137	Autumn 2013	19
PROBABILISTIC FORECASTING & MARINE ASPECTS			
Twenty-one years of wave forecast verification	150	Winter 2016/17	31
Hungary's use of ECMWF ensemble boundary conditions	148	Summer 2016	24
What conditions led to the Draupner freak wave?	148	Summer 2016	37
Using ensemble data assimilation to diagnose flow-dependent forecast reliability	146	Winter 2015/16	29
Have ECMWF monthly forecasts been improving?	138	Winter 2013/14	18
Closer together: coupling the wave and ocean models	135	Spring 2013	6
METEOROLOGICAL APPLICATIONS & STUDIES			
'L'alluvione di Firenze del 1966': an ensemble-based re-forecasting study	148	Summer 2016	31
Diagnosing model performance in the tropics	147	Spring 2016	26
NWP-driven fire danger forecasting for Copernicus	147	Spring 2016	34
Improvements in IFS forecasts of heavy precipitation	144	Summer 2015	21
New EFI parameters for forecasting severe convection	144	Summer 2015	27
The skill of ECMWF cloudiness forecasts	143	Spring 2015	14
Calibration of ECMWF forecasts	142	Winter 2014/15	12
Twenty-five years of IFS/ARPEGE	141	Autumn 2014	22
Potential to use seasonal climate forecasts to plan malaria intervention strategies in Africa	140	Summer 2014	15
Predictability of the cold drops based on ECMWF's forecasts over Europe	140	Summer 2014	32
Windstorms in northwest Europe in late 2013	139	Spring 2014	22
Statistical evaluation of ECMWF extreme wind forecasts	139	Spring 2014	29
Flow-dependent verification of the ECMWF ensemble over the Euro-Atlantic sector	139	Spring 2014	34
iCOLT – Seasonal forecasts of crop irrigation needs at ARPA-SIMC	138	Winter 2013/14	30
Forecast performance 2013	137	Autumn 2013	13
An evaluation of recent performance of ECMWF's forecasts	137	Autumn 2013	15
Cold spell prediction beyond a week: extreme snowfall events in February 2012 in Italy	136	Summer 2013	31



Newsletter | Number 150 – Winter 2016/17

European Centre for Medium-Range Weather Forecasts

www.ecmwf.int